Deep-Sea Research II 65-70 (2012) 141–162

Contents lists available at SciVerse ScienceDirect

Deep-Sea Research II

journal homepage: www.elsevier.com/locate/dsr2

The relationship between sea ice break-up, water mass variation, chlorophyll biomass, and sedimentation in the northern Bering Sea

L.W. Cooper [a,*], M.A. Janout [b,1], K.E. Frey [c], R. Pirtle-Levy [d], M.L. Guarinello [a], J.M. Grebmeier [a], J.R. Lovvorn [e]

[a] Chesapeake Biological Laboratory, University of Maryland Center for Environmental Science, PO Box 38, Solomons, MD 20688, USA
[b] School of Fisheries and Ocean Science, University of Alaska Fairbanks, Fairbanks, AK 99775, USA
[c] Graduate School of Geography, Clark University, 950 Main Street, Worcester, MA 01610, USA
[d] Department of Marine, Earth and Atmospheric Sciences, Campus Box 8208, North Carolina State University, Raleigh, NC 27695-8208, USA
[e] Department of Zoology, Southern Illinois University, Carbondale, IL 62901, USA

ARTICLE INFO

Available online 8 February 2012

Keywords:
Sedimentation
Arctic zone
Ice cover
Ice breakup
Bering Sea

ABSTRACT

The northern Bering Sea shelf is dominated by soft-bottom infauna and ecologically significant epifauna that are matched by few other marine ecosystems in biomass. The likely basis for this high benthic biomass is the intense spring bloom, but few studies have followed the direct sedimentation of organic material during the bloom peak in May. Satellite imagery, water column chlorophyll concentrations and surface sediment chlorophyll inventories were used to document the dynamics of sedimentation to the sea floor in both 2006 and 2007, as well as to compare to existing data from the spring bloom in 1994. An atmospherically-derived radionuclide, ^{7}Be, that is deposited in surface sediments as ice cover retreats was used to supplement these observations, as were studies of light penetration and nutrient depletion in the water column as the bloom progressed. Chlorophyll biomass as sea ice melted differed significantly among the three years studied (1994, 2006, 2007). The lowest chlorophyll biomass was observed in 2006, after strong northerly and easterly winds had distributed relatively low nutrient water from near the Alaskan coast westward across the shelf prior to ice retreat. By contrast, in 1994 and 2007, northerly winds had less northeasterly vectors prior to sea ice retreat, which reduced the westward extent of low-nutrient waters across the shelf. Additional possible impacts on chlorophyll biomass include the timing of sea-ice retreat in 1994 and 2007, which occurred several weeks earlier than in 2006 in waters with the highest nutrient content. Late winter brine formation and associated water column mixing may also have impacts on productivity that have not been previously recognized. These observations suggest that interconnected complexities will prevent straightforward predictions of the influence of earlier ice retreat in the northern Bering Sea upon water column productivity and any resulting benthic ecosystem re-structuring as seasonal sea ice retreats in the northern Bering Sea.

1. Introduction

Recent declines in Arctic seasonal sea ice make it imperative to understand the range of ecosystem responses to the climatic warming that seems to be clearly underway at high latitudes. For example, it is thought that declining sea ice coverage will increase light penetration and increase primary production on polar continental shelves (Arrigo et al., 2008), which might be globally significant because the continental shelves in the Arctic are the world's largest in extent. However, in comparing between chlorophyll biomass in the Bering Sea for two different years with light versus heavy ice coverage, open water conditions in early spring did not lead to significantly higher water column chlorophyll biomass (Clement et al., 2004) possibly because high winds can vertically mix phytoplankton in open water. Lomas et al. (2012) also point out that the high degree of spatial and temporal variability in biological productivity across the Bering Sea will make it challenging to detect shifts in production that can be attributed solely to declining seasonal sea ice. Consequently it is uncertain if declining sea ice will by itself lead to greater biological production on subarctic shelves despite a greater access to light when ice cover is diminished.

Another potentially important factor impacting the Arctic ecosystem in a declining seasonal sea ice regime is the timing of seasonal sea ice retreat. Currently, the northern Bering and Chukchi continental shelves have short food chains that deposit organic material synthesized during the brief, but intense production period directly to the shallow sea floor without much utilization by zooplankton (Cooper et al., 2002; Lovvorn et al., 2005).

* Corresponding author. Tel.: +1 410 326 7359.
E-mail address: cooper@umces.edu (L.W. Cooper).
[1] Present address: Alfred-Wegener-Institut, P.O. Box 12 01 6127515 Bremerhaven, Germany.

0967-0645/$ - see front matter © 2012 Elsevier Ltd. All rights reserved.
doi:10.1016/j.dsr2.2012.02.002

Specialized apex predators such as walrus, gray whales, bearded seals and diving sea ducks exploit the rich benthos as a food resource, but there is also evidence that fish are becoming more important in structuring the food web (Cui et al., 2009; Grebmeier et al., 2006). Early retreat of sea ice and later phytoplankton bloom development is hypothesized to prompt better development of zooplankton, which may become more important in intercepting seasonal primary production and increasing the pelagic component of the food web (Hunt et al., 2002, 2011). Ecological plasticity on the part of higher trophic feeders may also lead to changes that further complicate understanding how the ecosystem will adjust as sea ice declines and habitat availability changes (e.g. Pyenson and Lindberg, 2011).

In part to address these uncertainties regarding the biological impacts from changes in seasonal sea ice coverage and duration, we present data here on satellite, water column and benthic observations made during two seasons of ice retreat in May–June of 2006 and 2007 on the northern Bering Shelf aboard the USCGC *Healy*. In July 2006 and 2007, follow-up sampling well after the spring bloom from the CCGS *Sir Wilfrid Laurier* facilitated observations of the ultimate fate of sea surface derived organic materials and proxy tracers.

Our sampling builds upon extensive ecological studies that have been undertaken in the Bering Sea, dating back to Processes and Resources of the Bering Sea Shelf (PROBES) in the 1970s (summarized by McRoy et al., 1986) and the Inner Shelf Transfer and Recycling (ISHTAR) program in the 1980s (summarized by McRoy, 1993), including studies of the biological bloom at the time of ice retreat (e.g. Niebauer, 1991; Niebauer et al., 1995). However, there have been only a handful of scientific observations undertaken on the productive northern shelf between St. Matthew Island and Bering Strait at the time of ice retreat, when an ice-associated phytoplankton bloom results in an annual maximum in phytoplankton biomass (Cooper et al., 2002). Our data in particular reflect upon the development and intensity of the bloom and the timing of transmission of particulates to the sea floor. Specifically we determined water column conditions such as salinity and water column structure, as well as concentrations of nutrients that support phytoplankton (i.e. chlorophyll production) in the water column. We also made successive determinations of the viable chlorophyll inventories present on surface sediments and the particle-reactive natural radionuclide ^{7}Be ($t_{1/2}=53$ d) as indicators for recent sedimentation. Because of the short half-life of this radionuclide, it is not present on the sea floor until after ice retreat (Cooper et al., 2005, 2009), so it is an indicator of recent particle deposition. Likewise, viable chlorophyll *a* inventories on surface sediments in the Bering Sea are at low levels at the end of the winter, but increase significantly during and following the spring bloom (Cooper et al., 2002), providing another marker of particle accumulation. The two years studied were compared with each other in addition to a third year, 1994, when early season biological data are also available.

Our intent was to determine what relationships existed between sea ice distributions and subsequent water column chlorophyll concentrations and if there might be predictable consequences for chlorophyll biomass as a result of particular water mass distributions or sea ice retreat. The northern Bering Sea from St. Matthew Island to Bering Strait is entirely continental shelf, so changes in biological productivity and sea ice dynamics would have direct impacts on benthic communities.

While the Bering Sea is in part de-coupled from seasonal sea ice trends in the Arctic as a whole (Stabeno et al., 2012), portions of the study area, particularly north of St. Lawrence Island, have also had significant declines in annual sea ice cover over the past 30 years (Brown et al., 2011), a characteristic shared with the adjoining Chukchi Sea (Grebmeier et al., 2010). Decadal biomass declines and changes in Bering Sea benthic communities are underway and clearly coupled to overall water column productivity (Grebmeier et al., 2006). Therefore in putting our work in a biogeochemical context, one of the key questions that arises is the relationship of overall productivity of this Arctic system to changing seasonal sea ice extent and duration, and specifically what is predictable about the transfer of organic materials to the benthos under different sea ice melt scenarios.

1.1. Hydrography

The nutrient distribution in the region surrounding St. Lawrence Island (SLI) is governed by the course and extent of the Anadyr Current (AC) from the western side of the Bering Sea. The AC has its origin in the deep Bering Sea and consists of waters, termed Anadyr Water (AW) that upwell onto the Bering shelf from the Bering Slope Current (Kinder et al., 1975; Wang et al., 2009). After the AC travels anticyclonically around the Gulf of Anadyr, it moves eastward, meets the western point of SLI, where it bifurcates into a minor southeastward branch along the south side of SLI and a major northward branch through Anadyr Strait (Clement et al., 2005; Danielson et al., 2006, 2011; Grebmeier and Cooper, 1995). The straits in the northern Bering Sea (Anadyr, Shpanberg, Bering Strait) are energetic and therefore regions of enhanced vertical mixing (Clement et al., 2005).

Another influence on the shelf is the dilute and nutrient-poor Alaska Coastal Water (ACW) to the east of AW. ACW consists of coastal runoff from the western Alaska mainland as well as waters advected through the Aleutian Island passes from the Gulf of Alaska via the Alaska Coastal Current (ACC) (Mordy et al., 2005). After entering the southeastern Bering Sea shelf, the swift ACC becomes less defined and spreads its waters across the shelf. The less distinct water mass with intermediate salinity, termed Bering Shelf Water (cf. Grebmeier et al., 1989) is found on the mid-shelf and carries characteristics of both AW and ACW.

The northern Bering Sea is a distinct ecosystem, more continental in climate than Bering Sea waters to the south due to the surrounding North American and Asian land masses and SLI. The close proximity of land in the northern Bering Sea also means that wind forcing in the winter has a strong influence on local sea ice boundaries and brine injection through polynya dynamics (Stringer and Groves, 1991). The extreme west-to-east gradient in decreasing nutrient concentrations (and associated salinity) strongly influences biological production, which is concentrated to the west on the northern shelf (Springer et al., 1996). The absence of any continental slope in the study area means that all biological production in the water column is either quickly contributed to the benthos or is advected northward through Bering Strait into the Arctic Ocean (Grebmeier and McRoy, 1989).

2. Methods

Samples were collected during two cruises of the USCGC *Healy* (7 May–6 June 2006 and 16 May–18 June 2007) during the spring bloom in each year over a wide area of the northern Bering Sea from south of SLI north to Bering Strait (Tables 1 and 2). The overall *Healy* cruise plan in both 2006 and 2007 took advantage of the icebreaker to sample many of the same stations south of SLI with a gap of one-to-two weeks. The object of this repeated sampling, hereafter referred to as Pass 1 (9 May 2006–19 May 2006 and 18 May–29 May 2007 and Pass 2 (28 May 2006–6 June 2006 and 5 June–11 June 2007) was to document changes in water column and sediment characteristics as the ice-edge bloom progressed each year (Figs. 1 and 2). A smaller sub-set of additional samples collected on the CCGS *Sir Wilfrid Laurier*

Table 1
HLY0601 station information.

Pass	Station number	Station name	Date	Latitude °N	Longitude °W	Depth (m)
1	1	NEC5	5/9/2006	61.389	−171.947	62
1	2	SEC5	5/9/2006	61.564	−172.899	66
1	3	SIL5	5/9/2006	61.720	−173.604	62
1	4	SWC5	5/10/2006	61.887	−174.375	67
1	5	VNG1	5/10/2006	62.007	−175.069	73
1	6	NWC5	5/10/2006	62.053	−175.190	75
1	7	DLN5	5/11/2006	62.166	−176.011	95
1	8	NWC4	5/11/2006	62.399	−174.583	68
1	9	NWC4A	5/11/2006	62.578	−174.177	63
1	10	VNG3	5/12/2006	62.573	−173.831	61
1	11	SWC4	5/12/2006	62.262	−173.713	62
1	12	SIL4	5/12/2006	62.079	−172.946	60
1	13	SEC4	5/12/2006	61.938	−172.224	57
1	14	NEC4	5/13/2006	61.783	−171.297	47
1	15	SIL3	5/13/2006	62.440	−172.318	53
1	16	POP4	5/13/2006	62.403	−172.690	58
1	17	SWC4A	5/13/2006	62.428	−173.404	63
1	18	SWC3	5/14/2006	62.581	−173.086	67
1	19	VNG3.5	5/14/2006	62.574	−173.559	60
1	20	CD1	5/14/2006	62.678	−173.390	64
1	21	VNG4	5/14/2006	62.755	−173.426	69
1	22	NWC3	5/15/2006	62.783	−173.873	72
1	23	DLN3	5/15/2006	62.902	−174.577	65
1	24	DLN4	5/15/2006	62.513	−175.303	72
1	25	NWC2.5	5/15/2006	63.036	−173.480	65
1	26	NWC2	5/16/2006	63.103	−173.164	72
1	27	DLN2	5/16/2006	63.282	−173.744	75
1	28	VNG5	5/16/2006	62.971	−172.989	68
1	29	SWC3A	5/17/2006	62.752	−172.683	58
1	30	POP3A	5/17/2006	62.571	−172.298	51
1	31	SEC2.5	5/17/2006	62.496	−171.841	48
1	32	SEC3	5/17/2006	62.286	−171.569	47
1	33	NEC3	5/18/2006	62.063	−170.624	50
1	34	NEC2	5/18/2006	62.440	−170.059	38
1	35	NEC2.5	5/18/2006	62.472	−170.918	43
1	36	SEC2	5/18/2006	62.612	−170.919	45
1	37	SIL2	5/19/2006	62.752	−171.672	50
1	38	SWC2	5/19/2006	62.928	−172.305	58
1	39	VNG5	5/19/2006	62.963	−172.978	67
1	40	NWC2	5/19/2006	63.118	−173.116	69
1	41	NWC2.5	5/19/2006	63.035	−173.455	72
1	42	DLN2	5/19/2006	63.266	−173.747	74
1	43	DLN0	5/20/2006	64.285	−171.611	50
1	44	KIV1	5/20/2006	64.234	−170.864	35
1	45	KIV2	5/20/2006	64.189	−170.116	39
1	46	KIV3	5/20/2006	64.134	−169.354	38
1	47	KIV4	5/21/2006	64.064	−168.615	35
1	48	KIV5	5/21/2006	64.010	−167.860	37
1	49	NOM5	5/21/2006	64.368	−168.042	37
1	50	NOM4	5/21/2006	64.351	−168.629	40
1	51	NOM3	5/21/2006	64.394	−169.279	41
1	52	NOM2	5/22/2006	64.421	−170.057	43
1	53	NOM1	5/22/2006	64.474	−170.831	43
1	54	RUS1	5/22/2006	64.685	−170.566	49
1	55	RUS2	5/22/2006	64.658	−169.934	46
1	56	RUS3	5/22/2006	64.675	−169.086	45
1	57	RUS4	5/23/2006	64.645	−168.127	35
1	58	RUS4A	5/23/2006	64.803	−169.007	47
1	59	KNG1	5/23/2006	64.953	−169.855	47
1	60	CPW1	5/23/2006	65.189	−169.664	46
1	61	KNG2	5/23/2006	64.997	−169.134	48
1	62	CPW2	5/24/2006	65.186	−169.007	54
1	63	KNG3	5/24/2006	64.989	−168.411	47
1	64	CPW3	5/24/2006	65.191	−168.391	48
1	65	LDI2	5/24/2006	65.424	−168.422	59
1	66	BRS-A8	5/24/2006	65.463	−167.853	27
1	67	BRS-A7	5/25/2006	65.482	−167.986	40
1	68	BRS-A6	5/25/2006	65.506	−168.136	40
1	69	BRS-A5	5/25/2006	65.516	−168.319	58
1	70	BRS-A4	5/25/2006	65.547	−168.455	62
1	71	BRS-A3	5/25/2006	65.553	−168.619	59
1	72	BRS-A2	5/25/2006	65.578	−168.779	54
1	73	BRS-A1	5/25/2006	65.609	−168.946	50
1	74	LDI3	5/25/2006	65.711	−168.913	46
1	75	LDI4	5/25/2006	65.665	−168.840	50

Table 1 (*continued*)

Pass	Station number	Station name	Date	Latitude °N	Longitude °W	Depth (m)
1	76	LDI1	5/25/2006	65.409	−168.989	55
1	77	SPH6	5/26/2006	64.316	−166.531	26
1	78	SPH5	5/26/2006	64.201	−166.813	32
1	79	SPH4	5/26/2006	64.049	−167.184	31
1	80	SPH3	5/26/2006	63.842	−167.598	35
1	81	SPH2	5/26/2006	63.684	−167.945	32
1	82	SPH1	5/27/2006	63.480	−168.291	29
1	83	NEC1	5/27/2006	62.750	−169.588	42
1	84	SEC1	5/27/2006	62.987	−170.261	30
1	85	SEC2	5/27/2006	62.613	−170.943	45
2	86	NEC-5A	5/28/2006	61.408	−171.996	60
2	87	SEC4	5/28/2006	61.938	−172.212	58
2	88	SIL4	5/28/2006	62.077	−172.944	57
2	89	POP4	5/28/2006	62.403	−172.690	58
2	90	SWC-3A	5/29/2006	62.757	−172.711	63
2	91	SWC-2B	5/29/2006	62.862	−172.248	57
2	92	SWC-2C	5/29/2006	62.983	−171.725	53
2	93	SWC-2D	5/29/2006	63.095	−171.294	50
2	94	SIL1	5/29/2006	63.166	−170.917	33
2	95	SWC1	5/29/2006	63.284	−171.673	49
2	96	VNG5	5/29/2006	62.973	−173.021	70
2	97	NWC2.5	5/29/2006	63.026	−173.469	71
2	98	NWC2	5/30/2006	63.104	−173.136	73
2	99	NWC1	5/30/2006	63.488	−172.353	52
2	100	ANS-A	5/30/2006	63.505	−172.566	55
2	101	ANS-B	5/30/2006	63.525	−172.717	58
2	102	ANS-C	5/31/2006	63.556	−172.897	63
2	103	DLN1	5/31/2006	63.573	−173.027	62
2	104	VNG4	5/31/2006	62.756	−173.426	70
2	105	CD1	5/31/2006	62.679	−173.377	67
2	106	SWC-4A	5/31/2006	62.414	−173.421	63
2	107	VNG3.5	5/31/2006	62.570	−173.592	67
2	108	NWC3	6/1/2006	62.780	−173.850	73
2	109	DLN3	6/1/2006	62.899	−174.552	80
2	110	NWC4	6/1/2006	62.396	−174.545	71
2	111	NWC5	6/1/2006	62.060	−175.207	80
2	112	VNG1	6/2/2006	62.024	−175.065	80
2	113	DBS-A	6/2/2006	62.020	−176.349	100
2	114	DBS-B	6/2/2006	61.611	−177.132	117
2	115	DBS-C	6/2/2006	61.234	−177.791	145
2	116	DBS-D	6/3/2006	60.837	−178.504	174
2	117	DBS-E	6/3/2006	60.505	−179.101	430
2	118	DBS-1	6/3/2006	60.047	−179.663	2366

Table 2
HLY0702 station information.

Pass	Station number	Station name	Date	Latitude °N	Longitude °W	Depth (m)
1	1	NEC5	5/18/2007	61.389	−171.951	62
1	2	SEC5	5/18/2007	61.573	−172.906	67
1	3	SIL5	5/18/2007	61.724	−173.605	71
1	4	SWC5	5/19/2007	61.885	−174.368	75
1	5	VNG1	5/19/2007	62.018	−175.061	80
1	6	NWC5	5/19/2007	62.063	−175.207	82
1	7	DLN5	5/19/2007	62.148	−176.028	96
1	8	DLN4	5/20/2007	62.513	−175.296	81
1	9	NWC4	5/20/2007	62.135	−175.979	74
1	10	NWC4A	5/20/2007	62.559	−174.180	72
1	11	VNG3	5/20/2007	62.548	−173.835	69
1	12	VNG3.5	5/20/2007	61.922	−172.159	67
1	13	SWC4A	5/21/2007	62.412	−173.434	63
1	14	SWC4	5/21/2007	62.243	−173.743	65
1	15	SIL4	5/21/2007	62.081	−172.940	58
1	16	SEC4	5/21/2007	61.929	−172.215	58
1	17	NEC4	5/22/2007	61.771	−171.314	57
1	18	NEC3	5/22/2007	62.057	−170.625	50
1	19	SEC3	5/22/2007	62.277	−171.565	47
1	20	SEC2.5	5/22/2007	62.500	−171.848	50
1	21	POP3A	5/23/2007	62.567	−172.290	51
1	22	SIL3	5/23/2007	62.431	−172.316	52
1	23	POP4	5/23/2007	62.399	−172.696	60
1	24	SWC3	5/23/2007	62.578	−173.086	65
1	25	CD1	5/24/2007	62.501	−171.850	68

Table 2 (*continued*)

Pass	Station number	Station name	Date	Latitude °N	Longitude °W	Depth (m)
1	26	VNG4	5/24/2007	62.749	−173.411	70
1	27	NWC3	5/24/2007	62.782	−173.886	74
1	28	DLN3	5/24/2007	62.896	−174.587	80
1	29	DLN2	5/25/2007	63.274	−173.751	76
1	30	NWC2.5	5/25/2007	63.040	−173.438	72
1	31	NWC2	5/25/2007	63.110	−173.175	70
1	32	VNG5	5/25/2007	62.965	−173.026	69
1	33	SWC3A	5/25/2007	62.753	−172.712	62
1	34	SWC2	5/26/2007	62.921	−172.288	56
1	35	SIL2	5/26/2007	62.755	−171.674	51
1	36	SEC2	5/26/2007	62.608	−170.949	46
1	37	NEC2.5	5/26/2007	62.471	−170.965	44
1	38	NEC2	5/27/2007	62.429	−170.057	38
1	39	NEC1.5	5/27/2007	62.609	−169.814	42
1	40	NEC1	5/27/2007	62.758	−169.589	44
1	41	SEC1	5/27/2007	62.997	−170.267	41
1	42	SIL1	5/27/2007	63.169	−170.918	36
1	43	SIL0A	5/27/2007	63.268	−170.804	30
1	44	SIL0B	5/27/2007	63.248	−171.174	38
1	45	SWC2D	5/27/2007	63.098	−171.302	50
1	46	SWC2C	5/27/2007	62.988	−171.729	55
1	47	SWC1	5/28/2007	63.294	−171.708	52
1	48	NWC1	5/28/2007	63.498	−172.373	53
1	49	ANSA	5/28/2007	63.506	−172.574	56
1	50	ANSB	5/28/2007	63.528	−172.705	58
1	51	ANSC	5/28/2007	63.559	−172.889	61
1	52	DLN1	5/28/2007	63.507	−172.581	66
1	53	DLN0B	5/28/2007	63.805	−172.565	50
1	54	DLN0A	5/29/2007	64.035	−172.098	53
1	55	DLN0	5/29/2007	64.591	−171.611	51
1	56	KIV1	5/29/2007	64.225	−170.858	36
1	57	KIV2	5/29/2007	64.174	−170.091	37
1	58	KIV3	5/29/2007	64.126	−169.341	38
1	59	KIV4	5/29/2007	64.066	−168.618	36
1	60	KIV5	5/30/2007	64.019	−167.874	40
1	61	NOM5	5/30/2007	64.361	−168.033	37
1	62	NOM4	5/30/2007	64.364	−168.644	41
1	63	NOM3	5/30/2007	64.379	−169.286	40
1	64	NOM2	5/31/2007	64.422	−170.072	45
1	65	NOM1	5/31/2007	64.471	−170.849	46
1	66	RUS1	5/31/2007	64.692	−170.588	49
1	67	RUS2	5/31/2007	64.662	−169.941	47
1	68	RUS3	6/1/2007	64.676	−169.102	48
1	69	RUS4	6/1/2007	64.647	−168.127	36
1	70	KNG3	6/1/2007	65.013	−168.420	48
1	71	RUSA	6/1/2007	64.805	−169.026	46
1	72	KNG2	6/2/2007	64.991	−169.139	50
1	73	KNG1	6/2/2007	64.955	−169.886	44
1	74	CPW1	6/2/2007	65.182	−169.662	45
1	75	CPW2	6/2/2007	65.176	−169.042	52
1	76	CPW3	6/2/2007	65.182	−168.393	50
1	77	LDI2	6/3/2007	65.418	−168.430	61
1	78	BRSA-8	6/3/2007	65.445	−167.847	30
1	79	BRSA-7	6/3/2007	65.468	−167.972	40
1	80	BRSA-6	6/3/2007	65.493	−168.107	37
1	81	BRSA-5	6/3/2007	65.501	−168.287	54
1	82	BRSA-4	6/3/2007	65.529	−168.444	60
1	83	BRSA-3	6/3/2007	65.544	−168.649	57
1	84	BRSA-2	6/3/2007	65.566	−168.793	52
1	85	BRSA-1	6/3/2007	65.595	−168.950	50
1	86	LDI-A	6/3/2007	65.732	−168.947	33
1	87	ACW1	6/4/2007	65.113	−168.110	48
1	88	ACW2	6/4/2007	64.928	−167.552	32
1	89	ACW3	6/4/2007	64.678	−167.159	30
1	90	ACW4	6/4/2007	64.499	−166.851	27
1	91	SPH6	6/4/2007	64.323	−166.522	27
1	92	SPH6A	6/4/2007	64.446	−165.430	23
1	93	SPH6B	6/4/2007	64.384	−166.010	26
1	94	SPH5	6/4/2007	64.200	−166.797	32
1	95	SPH4	6/4/2007	64.040	−167.183	44
1	96	SPH3	6/4/2007	63.849	−167.608	33
1	97	YUK1	6/4/2007	63.977	−171.006	28
1	98	YUK2	6/5/2007	63.332	−167.209	26
1	99	YUK3	6/5/2007	63.014	−166.993	35
1	100	YUK4	6/5/2007	63.069	−167.440	36
1	101	YUK5	6/5/2007	63.110	−167.834	33

Table 2 (*continued*)

Pass	Station number	Station name	Date	Latitude °N	Longitude °W	Depth (m)
1	102	YUK6	6/5/2007	63.349	–168.096	29
1	103	SPH1	6/5/2007	63.501	–168.312	29
1	104	NSL4	6/5/2007	63.795	–168.733	34
1	105	NSL3	6/5/2007	63.863	–169.484	35
1	106	NSL2	6/5/2007	63.928	–170.252	39
1	107	NSL1	6/5/2007	63.979	–171.006	29
2	108	DLN0A	6/6/2007	64.031	–172.100	49
2	109	NWC2	6/6/2007	63.115	–173.137	71
2	110	VNG5	6/6/2007	62.971	–172.979	66
2	111	NWC2.5	6/6/2007	63.028	–173.432	72
2	112	NWC3	6/6/2007	62.780	–173.879	74
2	113	VNG4	6/7/2007	62.752	–173.401	70
2	114	CD1	6/7/2007	62.674	–173.360	68
2	115	VNG3.5	6/7/2007	62.570	–173.567	68
2	116	SWC3	6/7/2007	62.579	–173.079	63
2	117	POP4	6/8/2007	62.403	–172.691	60
2	118	SEC2.5	6/8/2007	62.492	–171.838	49
2	119	SEC3	6/8/2007	62.286	–171.565	47
2	120	NEC2.5	6/8/2007	62.470	–170.957	45
2	121	NEC2	6/8/2007	62.431	–170.064	39
2	122	NEC1.5	6/9/2007	62.613	–169.810	40
2	123	NEC1	6/9/2007	62.760	–169.579	40
2	124	MK1	6/9/2007	62.748	–168.962	34
2	125	MK2	6/9/2007	62.749	–168.400	34
2	126	MK3	6/9/2007	62.739	–167.840	27
2	127	MK4	6/9/2007	62.738	–167.262	36
2	128	MK5	6/9/2007	62.736	–166.583	25
2	129	MK6	6/9/2007	62.434	–166.864	30
2	130	MK7	6/9/2007	62.392	–167.377	42
2	131	MK8	6/9/2007	62.338	–167.892	32
2	132	MK9	6/9/2007	62.276	–168.416	32
2	133	MK10	6/9/2007	62.232	–168.937	36
2	134	MK10A	6/10/2007	62.476	–169.304	32
2	135	MK11	6/10/2007	62.179	–169.465	32
2	136	MK12	6/10/2007	62.112	–170.018	43
2	137	NEC3	6/10/2007	62.055	–170.632	49
2	138	SEC4	6/10/2007	61.927	–172.214	57
2	139	SEC5	6/11/2007	61.565	–172.921	70
2	140	SIL5	6/11/2007	61.725	–173.616	70
2	141	SWC5	6/11/2007	61.892	–174.364	77
2	142	VNG1	6/11/2007	62.019	–175.062	80
2	143	NWC5	6/12/2007	62.052	–175.198	83
2	144	DLN5	6/12/2007	62.147	–176.023	95
2	145	DLN4	6/12/2007	62.512	–175.300	80
2	146	NWC4	6/12/2007	62.389	–174.552	71
2	147	SWC4A	6/13/2007	62.413	–173.441	63
2	148	SWC3	6/13/2007	62.580	–173.079	65
2	149	VNG3.5	6/13/2007	62.571	–173.574	68
2	150	CD1	6/13/2007	62.675	–173.363	68
2	151	VNG4	6/13/2007	62.753	–173.411	69
2	152	VNG5	6/13/2007	62.966	–172.986	68
2	153	NWC2.5	6/13/2007	63.030	–173.442	72
2	154	DLN1	6/14/2007	63.579	–173.051	65
2	155	DL–A	6/14/2007	63.392	–173.472	74
2	156	DL-B	6/14/2007	63.212	–173.854	78
2	157	DL-C	6/14/2007	63.027	–174.236	77
2	158	DL-D	6/14/2007	62.848	–174.609	78
2	159	DL-E	6/14/2007	62.666	–174.987	70
2	160	DL–F	6/14/2007	62.486	–175.374	81
2	161	DL-G	6/14/2007	62.261	–175.844	72
2	162	DBS-A	6/14/2007	62.019	–176.340	100
2	163	DL-H	6/15/2007	61.826	–176.703	114
2	164	DBS-B	6/15/2007	61.611	–177.138	119
2	165	DL-I	6/15/2007	61.418	–177.445	129
2	166	DBS-C	6/15/2007	61.235	–177.786	148
2	167	DL-J	6/15/2007	61.034	–178.120	150
2	168	DBS-D	6/15/2007	60.836	–178.503	174
2	169	DL-K	6/15/2007	60.648	–178.839	228
2	170	DBS-E	6/15/2007	60.506	–179.101	438
2	171	DL-L	6/16/2007	60.284	–179.358	868
2	172	DBS-1	6/16/2007	60.025	–179.657	2420

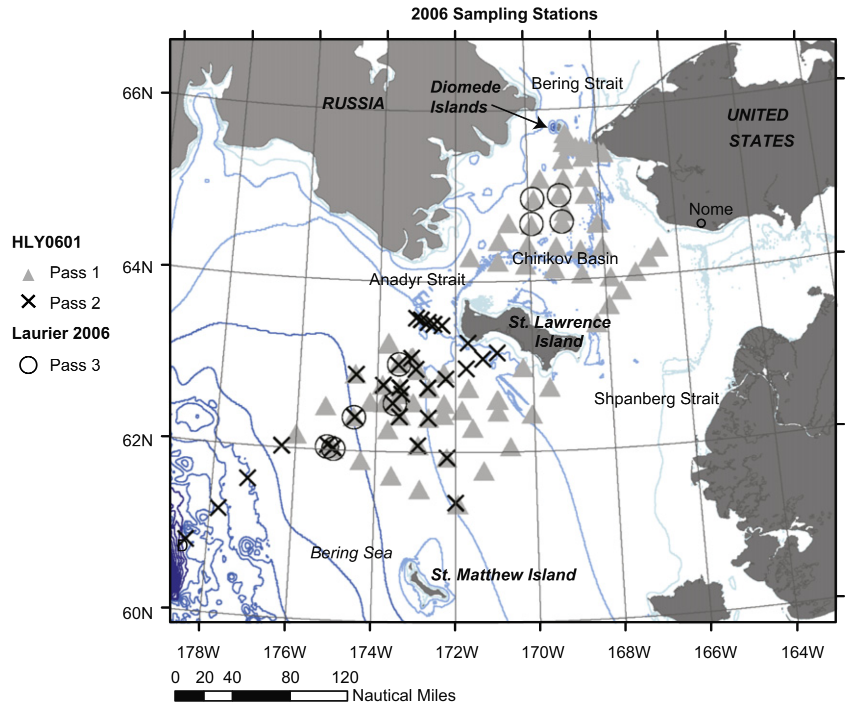

Fig. 1. Sampling locations in 2006, during cruises of the USCGC *Healy* and CCGS *Sir Wilfrid Laurier*.

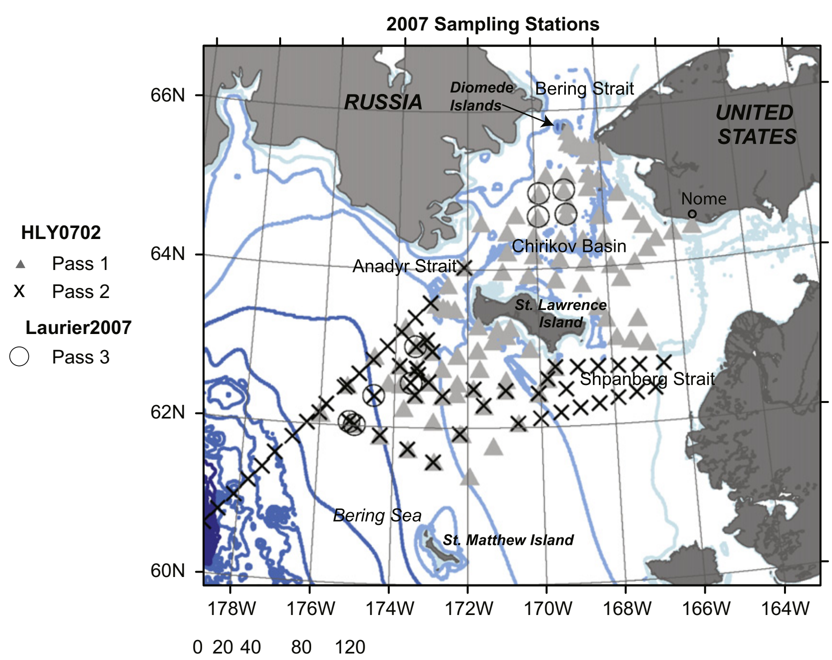

Fig. 2. Sampling locations in 2007, during cruises of the USCGC *Healy* and CCGS *Sir Wilfrid Laurier*.

(9–21 July 2006 and 9–20 July 2007) provided follow-up observations of mid-summer conditions (Tables 3 and 4). For comparison, we also used retrospective data from a 1994 cruise of the RV *Alpha Helix* (sampling from 8 May to 8 June 1994; additional details in Cooper et al., 2002).

The CTD rosette used aboard *Healy* consisted of a 12-place rosette with 30-L Niskin bottles and a Sea-Bird Electronics Model 911+ CTD system. Salinities were standardized with a Guildline Autosal salinometer with international seawater standards. The electronics system was calibrated before and after the cruises at the Sea-Bird manufacturing facility in Bellevue, Washington. For samples on the *Sir Wilfrid Laurier*, the CTD was a Sea-Bird SBE25/33 system mounted on a SBE32 Carousel 12-bottle water sampler with 8-L bottles.

Water collected from the Niskin bottles for nutrient analysis (nitrate+nitrite, ammonium, phosphate and silicate) was frozen shipboard in high-density polyethylene bottles. Following the cruise, the samples were shipped frozen to the Marine Science Institute, University of California, Santa Barbara and nutrient analysis was performed in using a Lachat Instruments QuikChem 800 nutrient analyzer.

Table 3
Sir Wilfrid Laurier 2006 station information.

Pass	Station number	Station name	Date	Latitude °N	Longitude °W	Depth (m)
3	39	SLIP1	7/12/2006	62.01	−175.05	80
3	40	SLIP2	7/12/2006	62.04	−175.22	82
3	41	SLIP3	7/12/2006	62.39	−174.57	67
3	42	SLIP5	7/13/2006	62.57	−173.55	66
3	43	SLIP4	7/13/2006	63.03	−173.46	73
3	45	UTBS5	7/14/2006	64.67	−169.92	47
3	46	UTBS2	7/14/2006	64.68	−169.09	46
3	47	UTBS4	7/14/2006	64.96	−169.88	49
3	48	UTBS1	7/14/2006	64.99	−169.14	49

Table 4
Sir Wilfrid Laurier 2007 station information.

Pass	Station number	Station name	Date	Latitude °N	Longitude °W	Depth (m)
3	32	SLIP1	7/13/2007	62.014	−175.056500	80
3	33	SLIP2	7/14/2007	62.05066667	−175.205000	82
3	34	SLIP3	7/14/2007	62.394	−174.569333	67
3	35	SLIP5	7/14/2007	62.56311667	−173.554050	74
3	36	SLIP4	7/14/2007	63.02898333	−173.456500	36
3	45	UTBS5	7/15/2007	64.6665	−169.921167	47
3	46	UTBS2	7/15/2007	64.683	−169.099	45
3	47	UTBS4	7/15/2007	64.95933333	−169.884500	49
3	48	UTBS1	7/15/2007	64.992	−169.136	47
3	62	UTN1	7/16/2007	66 42.5	−168 23.895	35
3	63	UTN2	7/17/2007	67 3.019	−168 43.885	47
3	64	UTN3	7/17/2007	67 20.061	−169 0.003	50
3	65	UTN4	7/17/2007	67 30.065	−168 54.604	50
3	66	UTN5	7/17/2007	67 40.222	−168 57.465	51
3	67	UTN6	7/17/2007	67 144.169	−168 26.298	50
3	68	UTN7	7/17/2007	67 59.944	−168 56.009	58
3	72	BC2	7/19/2007	71 24.75	−157 29.6	124
3	73	BC3	7/19/2007	71 34.7	−156 1.1	186
3	74	BC4	7/19/2007	71 55.8	−154 53.22	599

Optical characteristics of the water column, including Photosynthetic Active Radiation (PAR) and ultraviolet (UV) wavebands were measured at each station occupied during daylight hours with a calibrated Biospherical Instruments PUV510 submersible radiometer.

Water column chlorophyll was measured by filtering 250 mL water samples through 25 mm GF/F filters. The filters were initially frozen to fracture cell walls, and then stored in 10 mL of 90% acetone at 4 °C for 24 h in the dark. Extracted chlorophyll *a* extracted was measured using the Welschmeyer (1994) method with a Turner Designs 10-AU field fluorometer. The fluorometer was calibrated with a calibrated chlorophyll standard (Turner Designs Part No. 10-850) before and after all sampling, with use of a secondary solid standard (Part No. 10-AU-904) during sampling to identify any possible instrument drift. Integrated chlorophyll *a* was calculated for individual stations from ocean surface to sediments on a square meter basis, as most stations were 40–60 m in depth.

Surface sediment samples (0–1 cm) for ^{7}Be and chlorophyll *a* were collected on both cruises of the USCGC *Healy* during the spring bloom in 2006 and 2007. A smaller sub-set of additional samples collected on the CCGS *Sir Wilfrid Laurier* (9–21 July 2006 and 9–20 July 2007) provided follow-up observations of mid-summer conditions. Surface sediments samples collected at some sites on the cruises used a multi- or single-HAPS benthic corer (133 cm^2; Kanneworff and Nicolaisen, 1973) but most surface sediment samples were collected from the top of a van Veen grab (0.1 m^2) before it was opened. Prior studies have determined that for these shelf sediments, bioturbation is large enough that the less disturbed nature of surface sediments collected by corers relative to grabs is negated (Cooper et al., 1998; Pirtle-Levy et al., 2009).

Duplicate sediment cores for shipboard incubations were collected using a HAPS benthic corer with removable Plexiglas® insert sleeves (133 cm^2 surface area as described above). Under optimal conditions, the cores recovered were approximately 15 cm deep, with a low degree of apparent disturbance. Our criteria for determining low core disturbance during collection included the presence of clear water at the sediment–water interface, the presence of flocculent materials such as fecal pellets at the base of benthic burrows at the sediment surface, and continued filtering activity by macrobenthic invertebrates. Sediment–flux measurements for dissolved oxygen followed the methods of Grebmeier and McRoy (1989). Bottom water for these experiments was collected from the CTD rosette. Enclosed sediment cores with motorized paddles were maintained in the dark at in-situ bottom temperatures for approximately 12–24 h. Point measurements were made at the start and end of the experiment, and flux measurements were calculated, based on concentration differences adjusted to a daily flux per m^2. Previous shipboard measurements using real-time probe measurements in these cores indicated a steady decline in oxygen values in the overlying water during the course of the incubation. Sediments were sieved upon completing the experiment to normalize oxygen fluxes to infaunal biomass and to determine faunal composition (data to be reported elsewhere).

Surface sediment determinations of ^{7}Be were made on samples packed wet into 90 cm^3 cans. Corrections for efficiency and calibrations for all samples were made prior to counting with a mixed gamma standard traceable to the National Institute for Standards and Technology. Background corrections and control samples were analyzed prior to counting to verify detector performance. Some samples were off-loaded by helicopter prior to the end of the cruise, which facilitated all samples being analyzed within two half-lives of the date of collection. We used two shielded Canberra GR4020/S reverse electrode closed-end coaxial detectors that were at the time of analysis at the University of Tennessee, Knoxville. Sediment data reported have been decay-corrected to the date of collection. Data are reported as ^{7}Be detected, not detected, or trace amounts, which we defined as when counting errors were greater than 50%.

Surface sediment chlorophyll *a* inventories were measured using the Turner Designs fluorometer without acidification using a standardized method that includes a 12 h dark incubation in 90% acetone at 4 °C (Cooper et al., 2002). Surface sediment inventories reported are the mean of two independent determinations.

3. Results and discussion

For our results, we present first the water column data that documents the hydrography of the northern Bering Sea at the time of sampling, and the associated chlorophyll fields and nutrient distributions. Second, we address changes in the phytoplankton bloom that were observable during the course of each cruise, both in the water column, and in the benthic communities below. Third, we compare overall chlorophyll biomass among the three years for which data are available, and explore the relationships between available nutrients in each year and chlorophyll biomass. These analyses led us to finally document atmospheric forcing that influenced nutrient fields, sea ice formation and subsequent break-up.

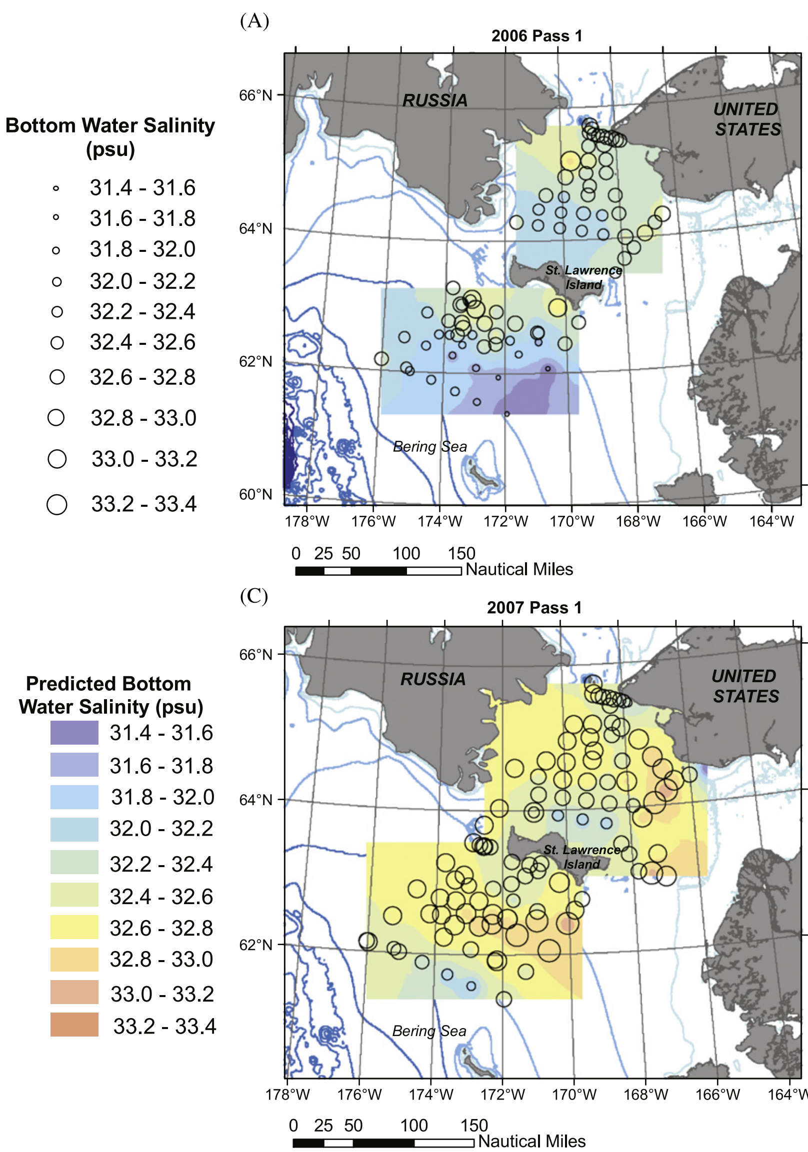

Fig. 3. Bottom water salinity in 2006 (A,B) and 2007 (C,D) for two separate occupations (termed Pass 1 and Pass 2) south of St. Lawrence Island, as well as intervening sampling north of St. Lawrence Island. Conditions were generally more saline in 2007. Pass 1: 9 May 2006–19 May 2006 and 18 May–29 May 2007; Pass 2: 28 May 2006–6 June 2006 and 5 June–11 June 2007. Symbols correspond to the available data; color gradations are estimated (predicted) interpolations and are created using inverse distance weighting method (default settings) of Geospatial Analyst Extension for ArcMap 9.3 (ESRI, Redlands, California).

3.1. Hydrography, nutrients and chlorophyll fields

During spring in the northern Bering Sea, near surface waters are highly variable in salinity and temperature as a result of strong impacts by local ice melt, surface warming and winds, while bottom water temperatures are often uniformly near the freezing point (< -1.5 °C). In large part for these reasons, we used bottom salinities to determine the water mass distribution. The location of geographical features mentioned in this section are shown in Figs. 1 and 2.

2006: In May–June 2006, the survey showed a comparatively large influence from fresher ACW (<32), during the two passes through the southern 2/3rds of the study area that was south of SLI (Fig. 3A and B). Consistent with the lower nutrient content of ACW, nitrate+nitrite concentrations were distinctly lower (0–3 μmol kg^{-1}) but showed a southeast-to-northwest gradient in increasing nitrate+nitrite (to 5–10 μmol kg^{-1}) in the higher salinity waters ($\sim$32.5) further west (Fig. 4A and B).

North of SLI, fresher waters (<32) were absent, which is not typical later in the summer when a strong west to east decreasing gradient in salinity develops as a result of peak seasonal runoff from major rivers on the North American mainland such as the Yukon (e.g. Danielson et al., 2011). However consistent with summer observations (e.g. see Walsh et al., 1989), the highest nitrate+nitrite concentrations (>10 μmol kg^{-1}; Fig. 4B) in 2006 were found just north of Anadyr Strait, where nutrient rich AW enters the Chirikov Basin that lies between SLI and Bering Strait. Turbulent vertical mixing occurs over the shallow Anadyr Strait, which is reflected in well-mixed water properties at the westernmost stations occupied, particularly to the north of SLI. Some stations close to SLI, occupied in early June (Pass 2, Fig. 3B) were impacted by the eastward branch of the AC flowing towards and along the south shore of the island, as reflected in the highest salinity ($\sim$33) waters found during the 2006 survey to the west of the island. Similarly, nitrate+nitrite concentrations were highest here (>12 μmol kg^{-1}). Bottom temperatures (Fig. 5A and B)

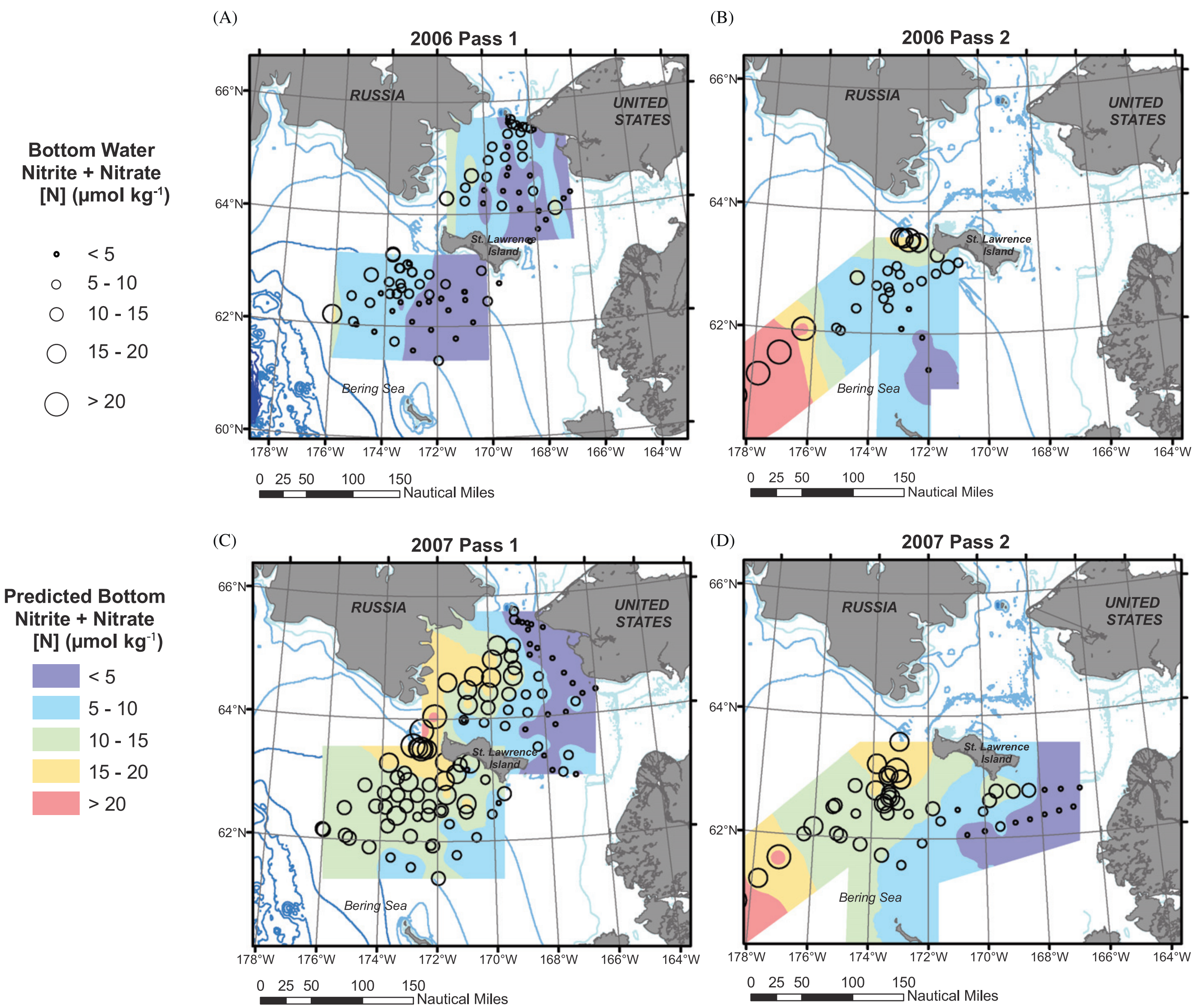

Fig. 4. Bottom water nitrate+nitrite (μM) in 2006 (A,B) and 2007 (C,D) for two separate occupations (termed Pass 1 and Pass 2) south of St. Lawrence Island, as well as intervening sampling north of St. Lawrence Island. Nitrate+nitrite (and other nutrient, data not shown, were generally higher in 2007. Pass 1: 9 May 2006–19 May 2006 and 18 May–29 May 2007; Pass 2: 28 May 2006–6 June 2006 and 5 June–11 June 2007. Symbols correspond to the available data; color gradations are estimated (predicted) interpolations and are created using inverse distance weighting method (default settings) of Geospatial Analyst Extension for ArcMap 9.3 (ESRI, Redlands, California).

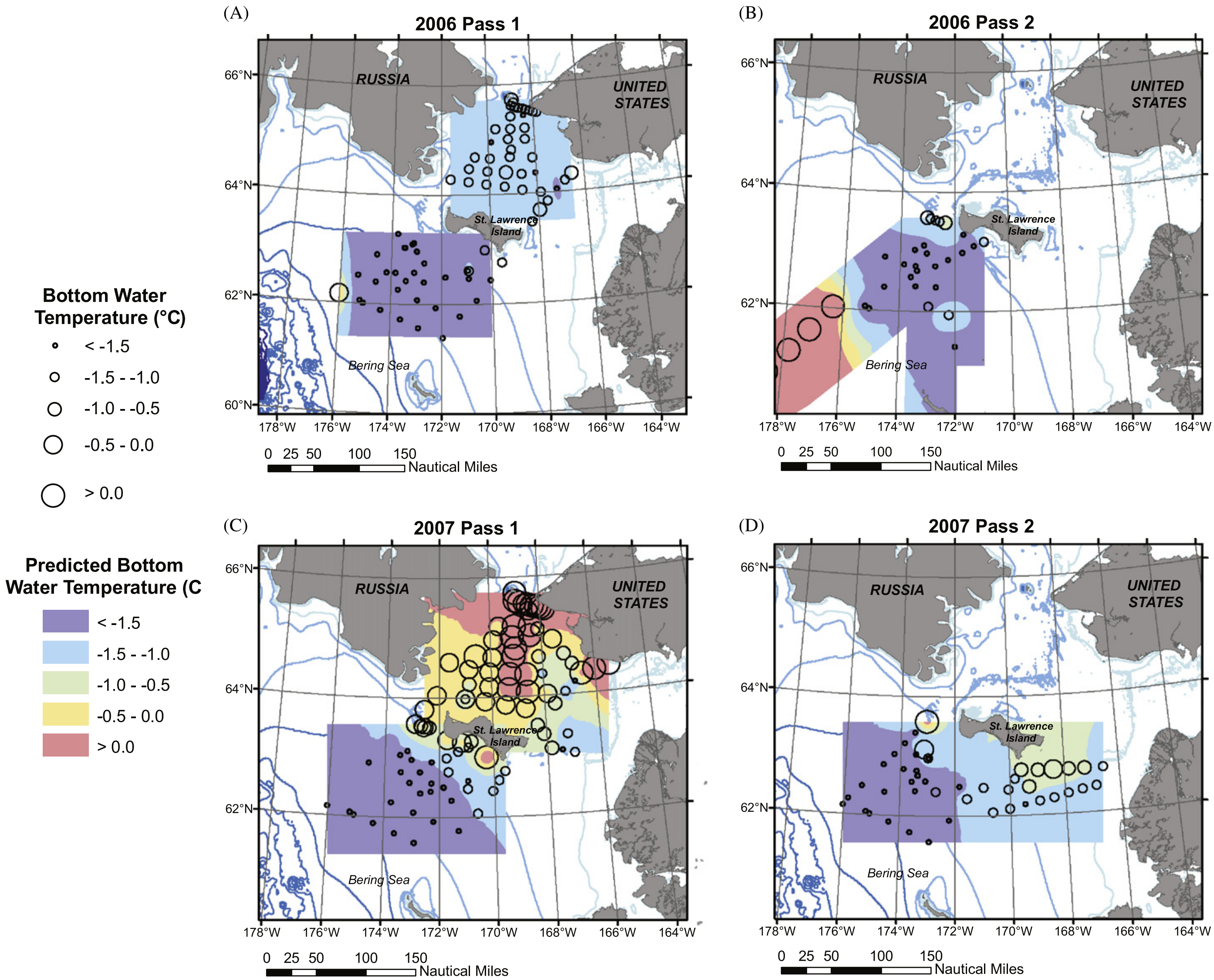

Fig. 5. Bottom water temperature in 2006 (A,B) and 2007 (C,D) for two separate occupations (termed Pass 1 and Pass 2) south of St. Lawrence Island, as well as intervening sampling north of St. Lawrence Island, Bering Sea. Pass 1: 9 May 2006–19 May 2006 and 18 May–29 May 2007; Pass 2: 28 May 2006–6 June 2006 and 5 June–11 June 2007. Symbols correspond to the available data; color gradations are estimated (predicted) interpolations and are created using inverse distance weighting method (default settings) of Geospatial Analyst Extension for ArcMap 9.3 (ESRI, Redlands, California).

were near the freezing point of seawater (<-1.6 °C) in most of the study area, although slightly warmer to the north of SLI (~-1 °C) and to the southwest of SLI (Pass 2; Fig. 5B) as sampling moved away from the ice-influenced area towards the deep Bering Sea at the end of the cruise. Phosphate and silicate values (not shown) followed a similar distribution as nitrate+nitrite (Fig. 4). With some exceptions to the north of SLI, nitrate+nitrite, silicate and phosphate generally followed the salinity trend as observed in prior summer sampling, with higher nutrient concentrations in more saline waters, and low nutrients in the fresher ACW. Surface nutrients by contrast were depleted over much of the area (data not shown), except in the well-mixed, high-energy region of Anadyr and Shpanberg Straits. Ammonium also varied from other nutrient distributions. It was generally found in higher concentrations south of SLI, but did not noticeably vary with water mass and was available even in nitrate-poor ACW to the south of the island (Fig. 6A and B). We also observed evidence that bottom water ammonium concentrations increased as the spring bloom progresses (Pass 1 versus Pass 2) over the whole study area (Fig. 6A and B), indicating mineralization of organic nitrogen from the sea floor in response to particle deposition.

The highest integrated chlorophyll values in 2006 ($\sim$1100 mg m^{-2}) were found south and west of SLI, as well as in large portions of the Chirikov Basin between SLI and Bering Strait (Fig. 7A and B). By and large, high-integrated chlorophyll fields coincided with elevated nutrient concentrations under the influence of the AC. Integrated chlorophyll concentrations were much lower ($<$100 mg m^{-2}) in the area occupied by low nutrient, low salinity ACW (Fig. 3A and B).

2007: The spring 2007 survey showed significantly different hydrographic conditions in the northern Bering Sea, when compared with 2006. An additional difference is that sampling was $\sim$10 days later, so some differences are due to the more mature spring bloom in 2007. For example, the higher ammonium concentrations in bottom waters in 2007 (Fig. 6C and D) than in 2006 (Fig. 6A and B) could reasonably be attributed to more of the bloom having reached the sea floor at the time of the 2007 sampling. The depth of the chlorophyll maximum was also lower

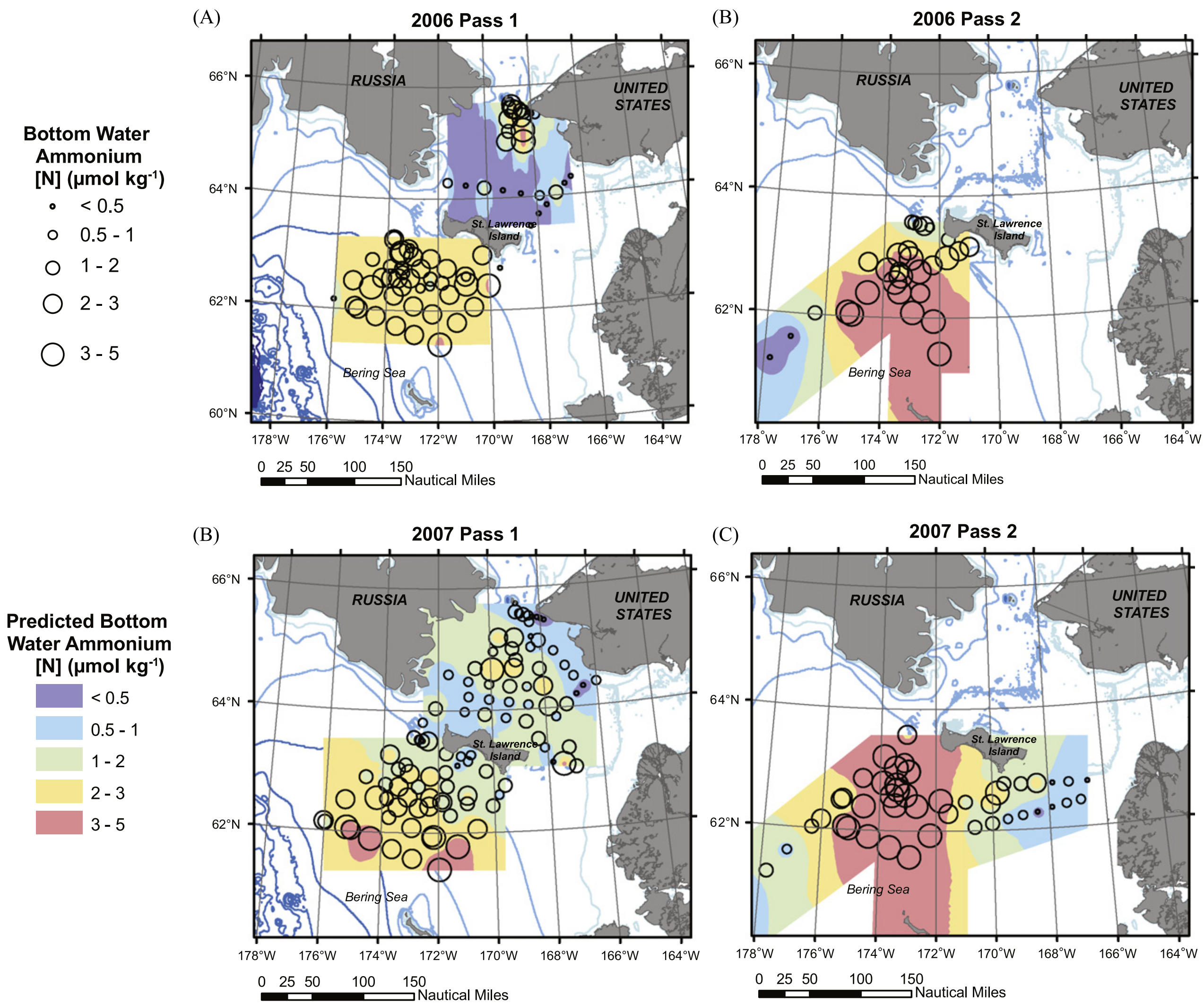

Fig. 6. Bottom water ammonium in 2006 (A,B) and 2007 (C,D) for two separate occupations (termed Pass 1 and Pass 2) south of St. Lawrence Island, as well as intervening sampling north of St. Lawrence Island, Bering Sea. Increases in ammonium in bottom water between Pass 1 and Pass 2 both years were interpreted as a result of increased benthic biological activity as the spring bloom reached the sea floor. Pass 1: 9 May 2006–19 May 2006 and 18 May–29 May 2007; Pass 2: 28 May 2006–6 June 2006 and 5 June–11 June 2007. Symbols correspond to the available data; color gradations are estimated (predicted) interpolations and are created using inverse distance weighting method (default settings) of Geospatial Analyst Extension for ArcMap 9.3 (ESRI, Redlands, California). Pass 1: 9 May 2006–19 May 2006 and 18 May–29 May 2007; Pass 2: 28 May 2006–6 June 2006 and 5 June–11 June 2007.

in the water column, particularly during Pass 2 in 2007 compared with 2006 (Fig. 9B and D). While widespread in 2006, low salinity water (< 32) was only found in few stations to the south of SLI in 2007 (Fig. 3C and D). In general, nutrient concentrations were also higher than in 2006 despite the generally later bloom development. The highest nitrate + nitrite concentrations (~20 μmol kg^{-1}) were observed where the AC bifurcates, one branch passing through Anadyr Strait and another branch of the current flowing along the south shore of SLI (Fig. 3C and D), with a salinity of 32.4–32.6. Another feature that was more intensively observed in 2007 relative to 2006 was high salinity (33–33.2) water spreading in an at least a 200-km-long band from Nome to southeast of SLI, and then extending in a westward tongue into the center of the study area to the south of SLI (Fig. 3C). In contrast to prior summer observations of high nutrient waters being correlated with more saline waters, bottom nitrate+nitrite in these saline waters was low (< 3 μmol kg^{-1}; Fig. 4C), suggesting the high salinity may simply have resulted from brine rejection during freezing of low nutrient ACW, possibly in late winter/early spring 2007, rather than the advection of more saline AW from the west. Bottom temperatures were low and near the freezing point of seawater (~ −1.6 °C) south of SLI in 2007, as in 2006 (Fig. 5) although some indications of bottom water warming can be seen. North of SLI, however in 2007, the western half of the Chirikov Basin had warmer (> −0.5 °C) bottom waters, with maximum temperatures (−0.5 to +0.5 °C) in a 200-km long, 50-km wide, well mixed band of water that extended due south from Bering Strait (Fig. 5C). Characteristics in this band also differed in other ways. These well-mixed waters had salinities of ~32.5, with significantly higher surface salinities relative to most other areas that were more obviously influenced by sea ice melting (data not shown). Higher bottom water nitrate+nitrite (> 10 μmol kg^{-1}) observed to the west, with continuous linkages to source waters in Anadyr Strait, were found in the southern half of this band (Fig. 4C). However, bottom nitrate+nitrite was lower (< 5 μmol kg^{-1}) to the east near the Alaskan coast (Fig. 4C), just to the east of the high chlorophyll concentrations (Fig. 7C) that were present in much of a well mixed, relatively warm water tongue (Fig. 5C).

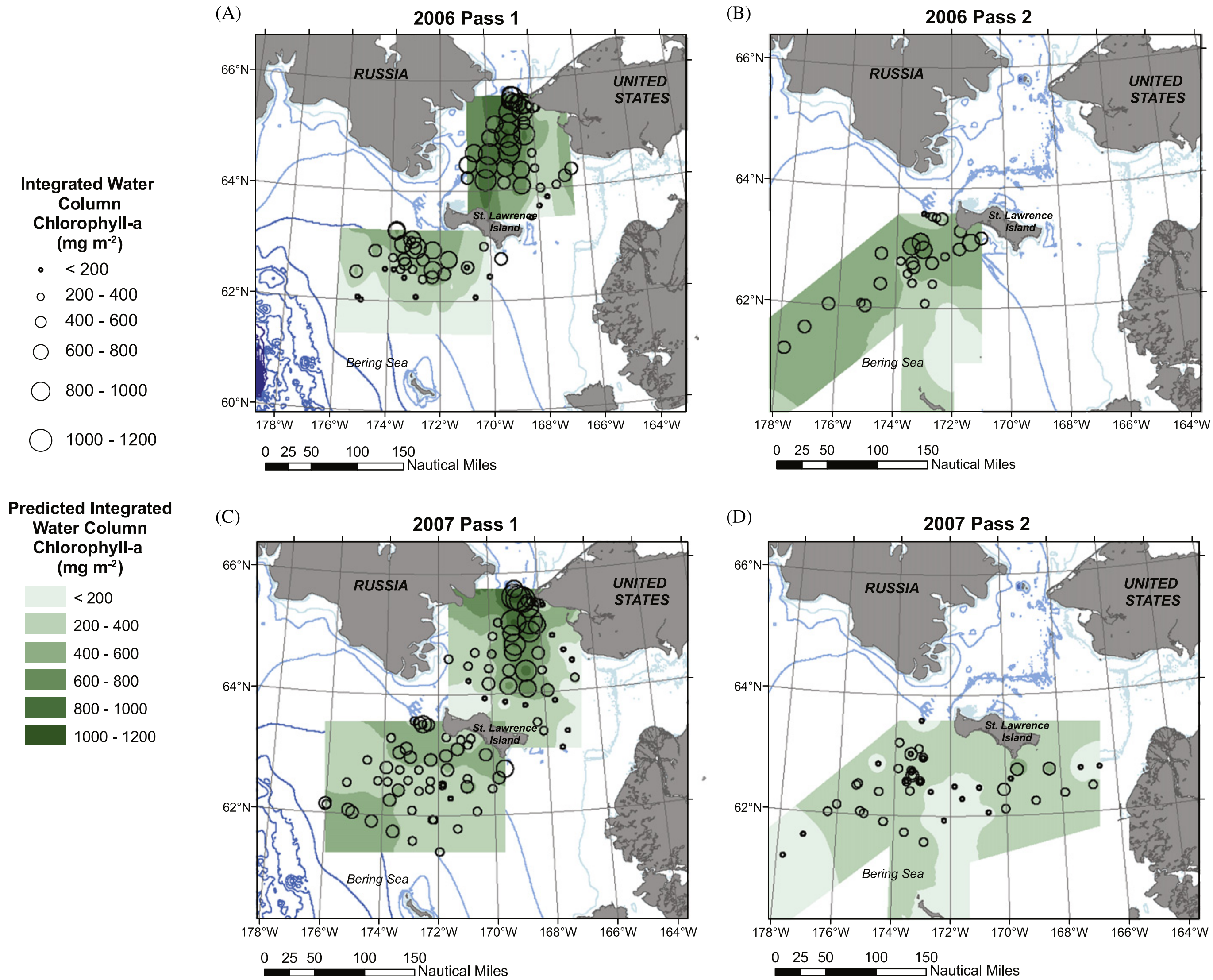

Fig. 7. Integrated chlorophyll *a* inventories (mg m^{-2}) in 2006 (A,B) and 2007 (C,D) for two separate occupations (termed Pass 1 and Pass 2) south of St. Lawrence Island, as well as intervening sampling north of St. Lawrence Island, Bering Sea. The integrated chlorophyll *a* inventories are based upon bottle measurements of chlorophyll *a* concentrations at discrete depths, which were summed from surface to seafloor. Symbols correspond to the available data; color gradations are estimated (predicted) interpolations and are created using inverse distance weighting method (default settings) of Geospatial Analyst Extension for ArcMap 9.3 (ESRI, Redlands, California).

3.2. Pass 1 versus Pass 2 dynamics

In both 2006 and 2007, the opportunity to replicate sampling at some of the same stations south of SLI over a two-to-three week time interval during spring production gave us the opportunity to document how conditions changed during a productive period over the shallow (~50 m) continental shelf. Within the water column, a few stations were sampled as many as three times during each cruise, with a classical ice-edge spring bloom proceeding as expected in most cases. For example, at two representative stations south of SLI (VNG3.5 and DLN 4; see Table 2 and Fig. 2 for location), each occupied three times in 2007, the later temporal sampling (Fig. 8A and B) showed increased surface water temperatures, increased density stratification mirroring salinity, and a fluorescence peak and oxygen maximum (both measured from the CTD) lowering to deeper depths (~40 m). The patterns observed were not always perfect. For example, at Station VNG3.5 (top panels of Fig. 8), the depth of chlorophyll maximum was actually lower on Day 159 than on a re-occupation of the same station six days later, but we expect that this represents horizontal advection of a chlorophyll maximum at different stages of development as sea ice locally broke up. The general pattern that was observed over the whole study area was for the depth of the chlorophyll maximum to deepen between Pass 1 and 2 in both years (Fig. 9) and the bloom was approaching near-bottom depths by the end of the sampling. This trend was particularly evident during 2007 (Fig. 9C and D), but sampling occurred ten days to two weeks later in 2007 than in 2006 (Fig. 9A and B). Although the oxygen sensor on the CTD profiler indicated that the dissolved oxygen maximum was often close to the chlorophyll maximum (e.g. Fig. 8A and B), we did not make primary production measurements that would confirm production in excess of respiration requirements. Optical measurements in the water column during the later sampling often indicated that the chlorophyll maxima were being observed at water depths where PAR was less than what is thought to be the shade-adapted compensation depth for marine microalgae in Arctic waters (~10 μE m^{-2} s^{-1}; Cota and Smith, 1991). For example, at Station DLN 1, occupied on 14 June 2007, the chlorophyll maximum was observed at 30 m, approximately 10 m below the apparent shade-adapted compensation depth as determined using the Biospherical Instruments PAR sensor

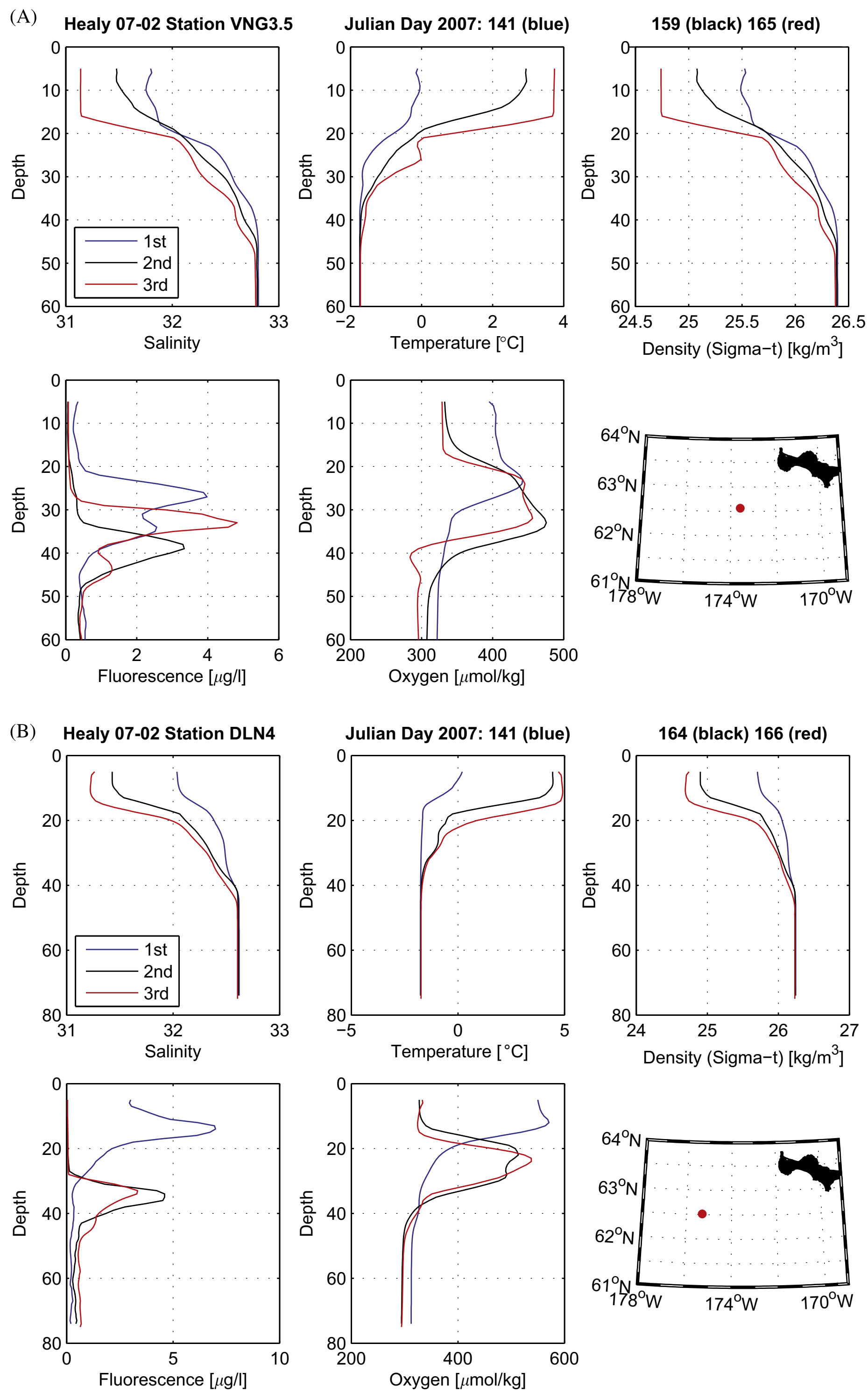

Fig. 8. A and B. Salinity, temperature, density, fluorescence, and dissolved oxygen profiles as measured from the CTD profiler at two representative stations (VNG3.5; (A) and DLN 4; (B)), each occupied three times in 2007, showing progressive changes in water column properties following ice dissolution. The three Julian dates of sampling are provided in the upper right hand corner of each sub-figure: 141, 159, 165 (blue, black, red, respectively, A) and 141, 164, and 166, (blue, black, red, respectively, B). (For interpretation of the references to colour in this figure legend, the reader is referred to the web version of this article.)

(Fig. 10). Of course, the estimate of Cota and Smith (1991) corresponds to the long-term photon flux required to sustain photosynthesis, but our station measurements were made at mid-day, under sunny conditions here and often at other stations. Our profiles generally correspond to high light conditions and we commonly observed that the chlorophyll maximum was at depths below the apparent shade-adapted compensation depth. The dissolved oxygen maximum often associated with the chlorophyll peak (e.g. Fig. 8) indicated apparent active production and not simply a sinking, senescent bloom.

The development and sinking of the phytoplankton bloom as measured via water column chlorophyll was also reflected in the

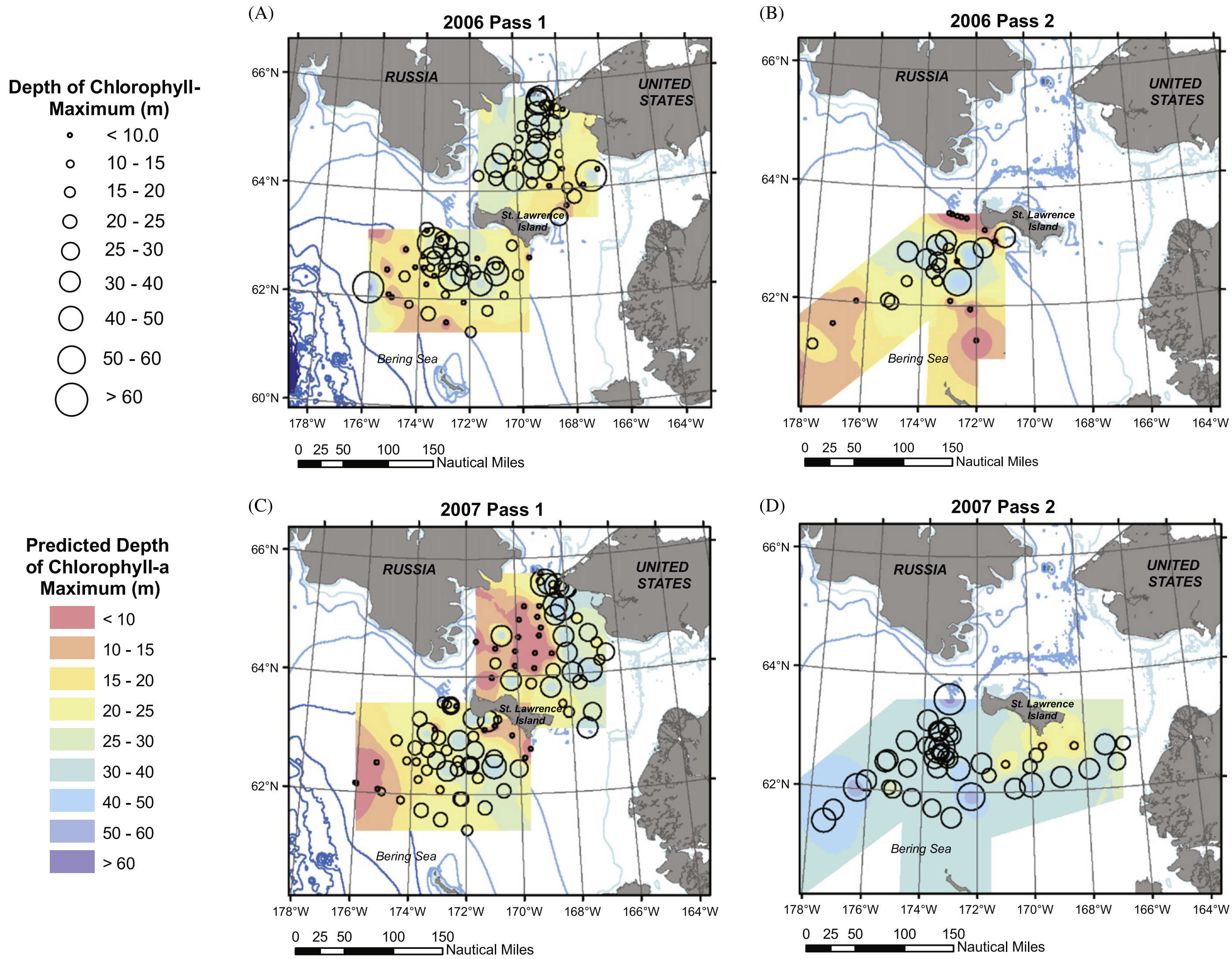

Fig. 9. The depth of the chlorophyll maximum as determined from the fluorescence sensor on the CTD 2006 (A,B) and 2007 (C,D), during two separate occupations (termed Pass 1 and Pass 2) south of St. Lawrence Island, as well as intervening sampling north of St. Lawrence Island. Pass 1: 9 May 2006–19 May 2006 and 18 May–29 May 2007; Pass 2: 28 May 2006–6 June 2006 and 5 June–11 June 2007. Symbols correspond to the available data; color gradations are estimated (predicted) interpolations and are created using inverse distance weighting method (default settings) of Geospatial Analyst Extension for ArcMap 9.3 (ESRI, Redlands, California).

benthic data that were collected during the study. Comparisons of sediment chlorophyll measured in surface sediment in 2006 and 2007 indicated an increase between Pass 1 and Pass 2 (Fig. 11A–D). Surface sediment inventories of chlorophyll were also generally higher in 2007 relative to 2006, consistent with the later date of sampling in 2007. Community oxygen demand, as measured in shipboard cores was higher in many cases during Pass 2 than Pass 1 in both years (Fig. 12). Finally, ^{7}Be was detected in many surface sediments during both cruises and during the follow-up July sampling from the CCGS *Sir Wilfrid Laurier*, reflecting the quick transmission of the radioisotope from its atmospheric origin to particles on the sea ice or open water surface (Fig. 13). Nevertheless it was less clear that there were consistent sequential increases in ^{7}Be inventories between Pass 1 and Pass 2 and the third sampling effort from the *Sir Wilfrid Laurier*. Deposition of the radionuclide was not observed in samples collected north of SLI, but south of Bering Strait (Chirikov Basin), which is consistent with previous observations in this area (Cooper et al., 2005) and the larger grain sediments and higher current flow regimes in the Chirikov Basin. The *Sir Wilfrid Laurier* sampling in mid-summer 2007 in particular suggested that sedimentation of the radionuclide occurs in three zones of the Bering and Chukchi Seas that have been previously identified as high deposition zones for soft sediments: (Grebmeier et al., 2006), i.e. southwest of SLI, just north of Bering Strait where currents subside and at the head of Barrow Canyon (also in the Chukchi Sea). However, deposition patterns of the radionuclide do not coincide entirely with indications from biological sedimentation (e.g. Figs. 11 and 12), so as has been suggested elsewhere (Cooper et al., 2005, 2009), sedimentation of this particle-reactive radionuclide during sea ice break-up is not tightly tied to biological activity.

3.3. *Summary of similarities and differences, 2006–2007 ice-edge blooms*

In general, the 2006 and 2007 ice edge blooms in the northern Bering Sea were qualitatively similar. As the bloom progressed, melted sea ice and surface warming led to stratification of the upper water column overlying a high biomass of chlorophyll that sank slowly in the water column. Within 2–3 weeks, the maximum chlorophyll concentration was at depths that appeared to be below compensation depths for typical marine phytoplankton, and sediment-based processes such as increased oxygen demand,

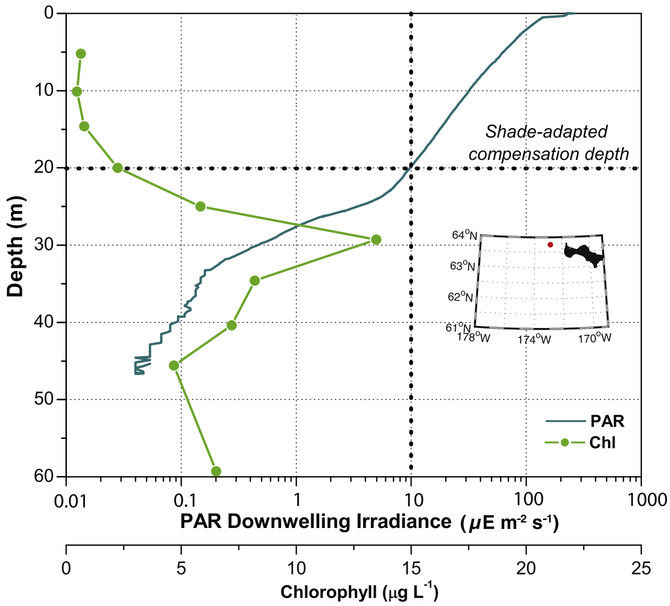

Fig. 10. Photosynthetic active radiation, measured by profiling radiometer and chlorophyll concentrations as directly measured from rosette bottles at a representative station, DLN1, occupied on 14 June 2007.

ammonium regeneration in bottom waters, and sedimentation of chlorophyll to the sediment surface increased. However, quantitatively the intensity of the chlorophyll bloom in each year differed spatially and significantly where it was possible to make direct comparisons south of SLI. While the highest integrated chlorophyll biomass was observed in both years near Bering Strait, in the waters south of SLI, higher inventories of chlorophyll (e.g. >600 mg m^{-2}) were more widely distributed in 2007 than in 2006 (Fig. 5). Both integrated chlorophyll biomass (in Pass 1) and bottom water nutrient concentrations were significantly higher in 2007 relative to 2006 (Table 5). The significant difference was determined by pair-wise comparisons of stations that were occupied both in 2006 and 2007 for waters south of SLI.

3.4. Chlorophyll and bottom water nitrate comparisons among three years

We also were able to compare these data from Pass 1 in 2006 and 2007 with previously published data from a third cruise in May 1994 aboard the RV *Alpha Helix* (Cooper et al., 2002) where that cruise also occupied many of the same stations. For the three years studied, 1994, 2006, and 2007, 26 stations were occupied on all three cruises at least once and in some cases twice in 2006 and 2007 (Table 5). All of these comparable stations were in waters

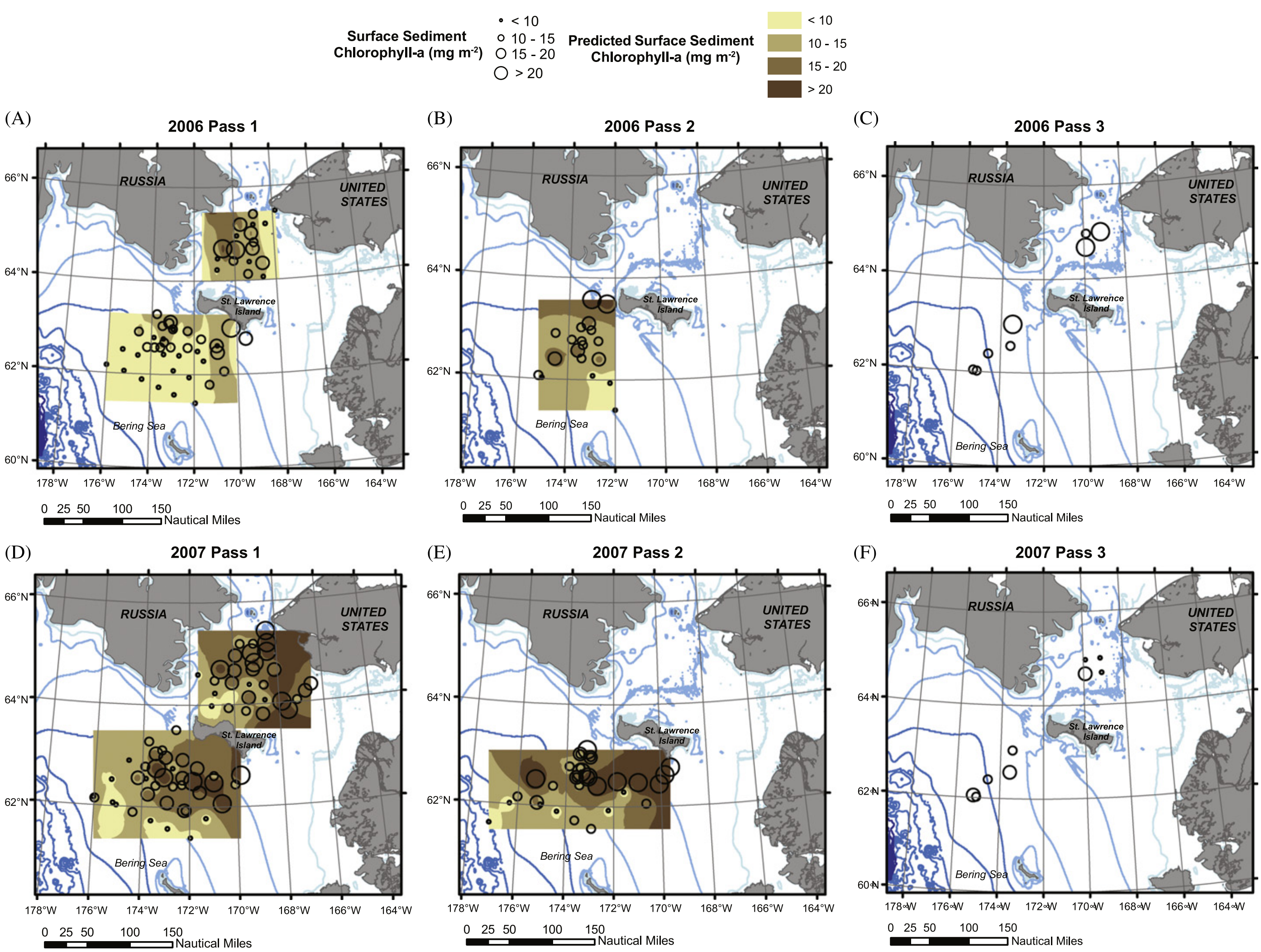

Fig. 11. Chlorophyll *a* inventories present in surface (0–1 cm) sediments, 2006 (A–C) and 2007 (D–F) during three separate occupations (termed Pass 1, Pass 2, and Pass 3) south of St. Lawrence Island, as well as intervening sampling north of St. Lawrence Island. Symbols correspond to the available data; color gradations are estimated (predicted) interpolations and are created using inverse distance weighting method (default settings) of Geospatial Analyst Extension for ArcMap 9.3 (ESRI, Redlands, California). Because of limited sampling from the *Sir Wilfrid Laurier* in July 2006 and 2007 no color interpolations are shown for Pass 3.

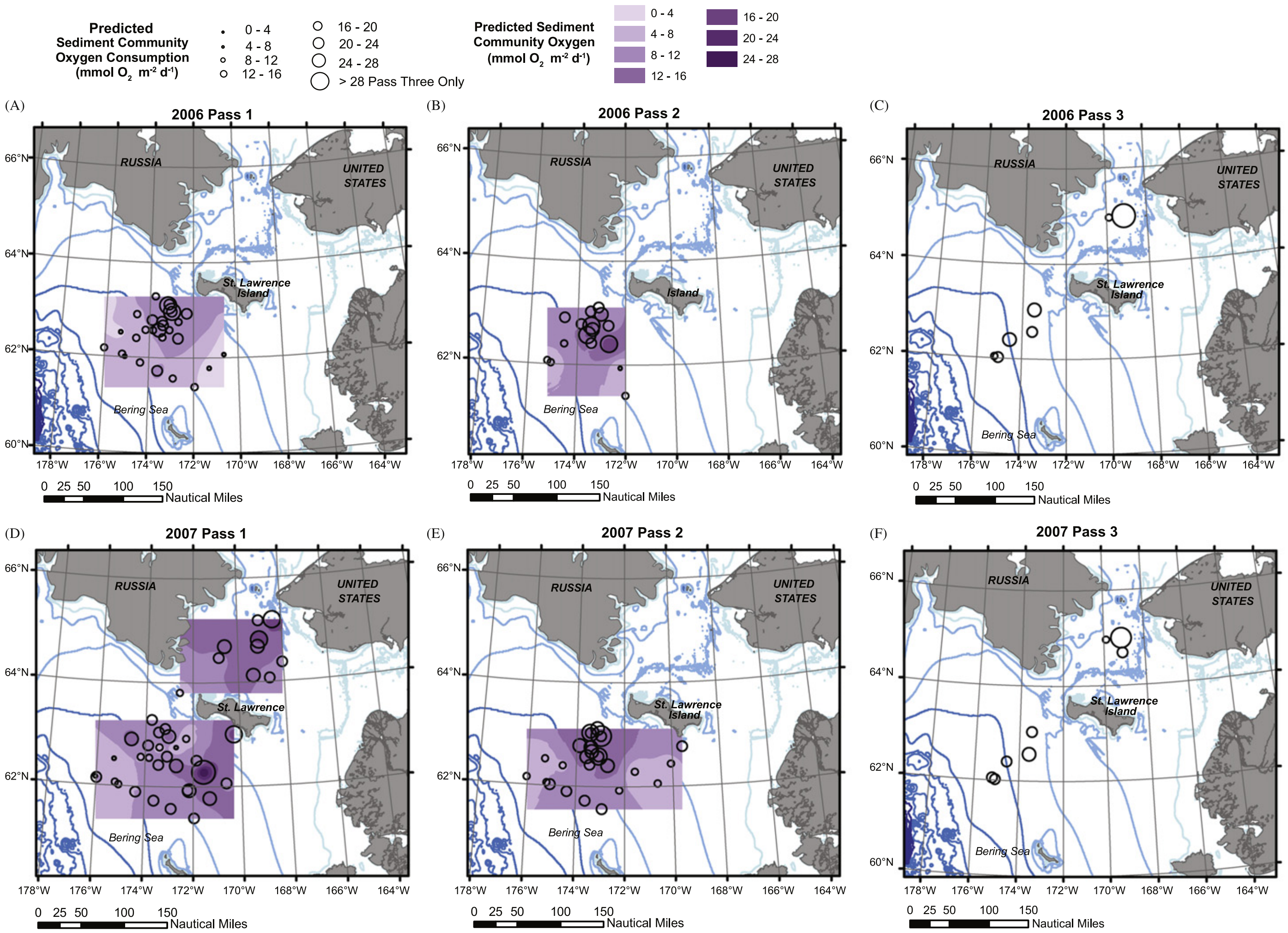

Fig. 12. Sediment oxygen consumption as measured in duplicate 133 cm^2 cores incubated shipboard for 12–24 h in both 2006 (A,B) and 2007 (C,D) during two sequential passes through the study area each year. Pass 1: 9 May 2006–19 May 2006 and 18 May–29 May 2007; Pass 2: 28 May 2006–6 June 2006 and 5 June–11 June 2007. Symbols correspond to the available data; color gradations are estimated (predicted) interpolations and are created using inverse distance weighting method (default settings) of Geospatial Analyst Extension for ArcMap 9.3 (ESRI, Redlands, California). Because of limited sampling from the *Sir Wilfrid Laurier* in July 2006 and 2007 no color interpolations are shown for Pass 3.

south of SLI. The mean integrated chlorophyll concentrations for the 26 stations occupied were significantly different each year (Table 6; paired t-tests, $p<0.05$), with highest mean chlorophyll biomass (south of SLI) observed in 1994 (557 mg m^{-2}), followed by 2007 (400 mg m^{-2}) with the lowest mean chlorophyll biomass observed in 2006 (246 mg m^{-2}). The small subset of stations re-sampled during Pass 2 south of the island in both 2006 and 2007 ($n=11$ and 13 respectively) in late May and early June also had lower mean chlorophyll biomass than observed in 1994 (Table 5). The differences in water column chlorophyll biomass inventories between 2006 and 2007 during late bloom sampling were not significant (paired t-test; $p>0.05$). It is worth noting that by the time of Pass 2 sampling in both 2006 and 2007, the chlorophyll maximum was below expected compensation depths and other indicators of sediment metabolism (e.g. oxygen respiration, bottom water ammonium, and sediment chlorophyll) reflected deposition of the bloom to the sea floor. It therefore seems reasonable to assume that the Pass 1 sampling comparison in May 2006 and 2007 better reflects the intensity of the bloom, which led to higher chlorophyll biomass in the waters south of SLI in 2007 than in 2006. Both years however lag behind the very high chlorophyll biomass observed in 1994, when water column inventories >1000 mg m^{-2} were observed south of SLI (Cooper et al., 2002). Chlorophyll biomass approached or exceeded 1000 mg m^{-2} in 2006 and 2007 only north of SLI, particularly in the immediate vicinity of Bering Strait, where turbulent mixing and remnant melting sea ice increased the overall water column inventory. Our interpretation of the high chlorophyll biomass near Bering Strait is that it includes dense chlorophyll concentrations derived from melting sea ice and the concentrations are higher than would be observed in the water column if contributions from melting ice were not present (K. Frey, unpublished satellite observations). This satellite imagery shows direct linkages between the intense phytoplankton blooms immediately south of Bering Strait in both 2006 and 2007 and remnant sea ice drifting north towards the Diomede Islands observed from satellites. Vertical mixing by currents in the Bering Strait also increases the areal inventory of chlorophyll from both sea ice and water column sources to very high levels.

Overall, patterns of chlorophyll biomass were linked to bottom water nitrate+nitrite concentrations, which were lowest in 2006 (Table 6), and higher in 1994 and 2007. Thus it seems reasonable to conclude that bottom water nitrate+nitrite concentrations are good predictors of the intensity of the phytoplankton bloom in

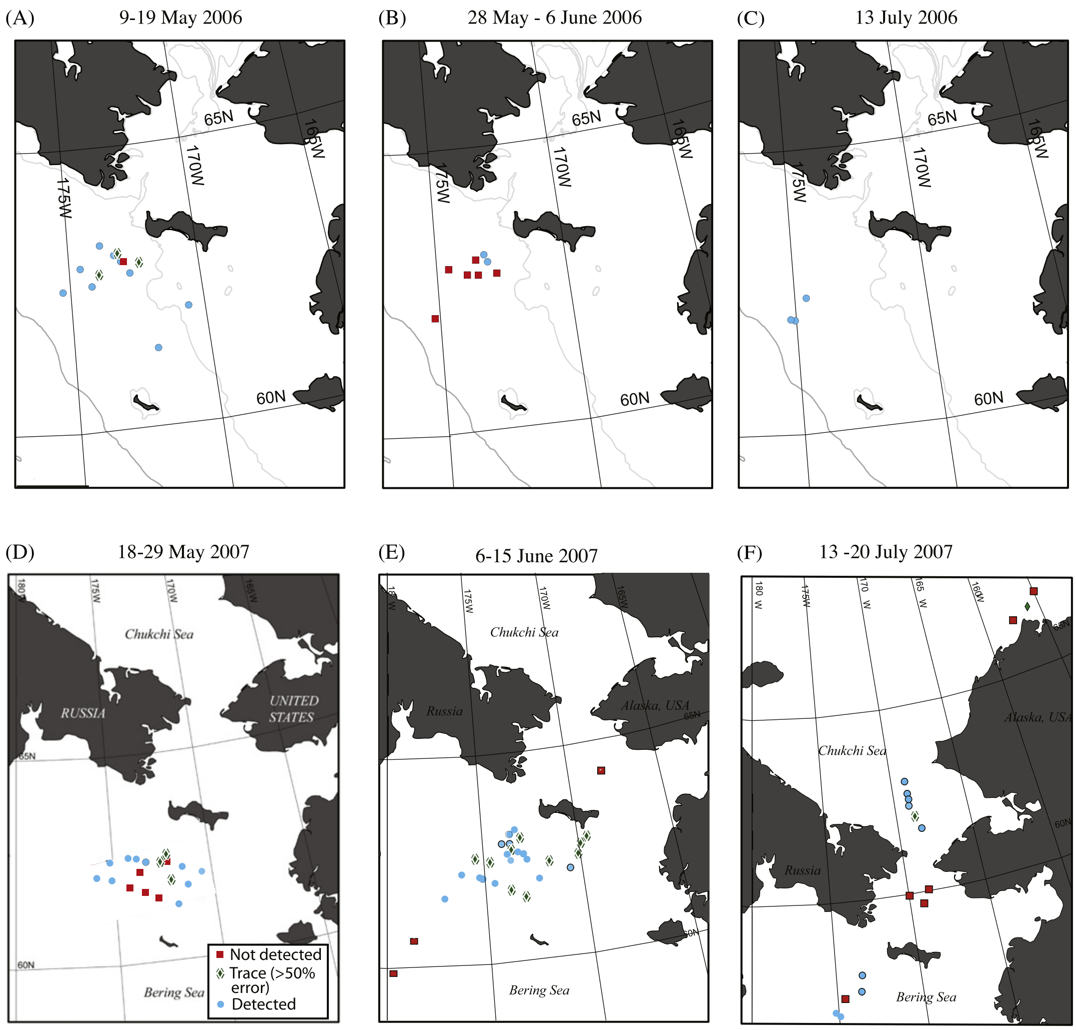

Fig. 13. (A–F) Presence of ^{7}Be (Bq m^{-2}) in surface sediments following ice retreat, 2006 and 2007 during sequential sampling each year.

Table 5
Mean ± SE for mean integrated chlorophyll (surface to seafloor) and bottom water nitrate + nitrite for stations compared south of Saint Lawrence Island, May 1994, 2006, 2007.

Sampling dates	Mean integrated chlorophyll *a* (mg m^{-2})	Mean bottom water nitrate + nitrite (μmol kg^{-1})	Number of stations
Ship platform			
RV *Alpha Helix*			
26 May – 6 June 1994	556.7 ± 52.5	10.70 ± 1.03	30
USCGC *Healy*			
9 – 19 May 2006	246.0 ± 49.5	6.42 ± 0.85	26
28 May – 6 June 2006	395.2 ± 61.8	8.32 ± 0.96	11
18 – 29 May 2007	400.4 ± 21.3	12.28 ± 1.45	30
5 – 11 June 2007	256.1 ± 20.6	12.04 ± 0.63	13

Table 6
Paired *t*-test results; 26-paired stations sampled on three cruises; May 1994 and Pass 1 on 2006 and 2007 *Healy* cruises.

t-Test comparison	Versus 2006	Versus 2007
Integrated chlorophyll *a*		
1994, *t*-ratio	4.934, $p < 0.001$	3.26, $p = 0.016$
2006, *t*-ratio		2.394, $p = 0.001$
Bottom nitrate + nitrite		
1994, *t*-ratio	6.529, $p < 0.001$	0.192, $p = 0.42$
2006, *t*-ratio		6.322, $p < 0.001$

any particularly year. We consider the importance of the timing of sea ice break-up as another factor in the following section.

3.5. Sea ice break-up

Satellite imagery was used to estimate timing of sea ice break-up (based on a 15% sea ice concentration threshold) in 1994, 2006, and 2007 (Fig. 14). For the greater northern Bering Sea region, each year varied, but 2007 had arguably earlier ice retreat over a larger area. The 26 stations where direct comparisons

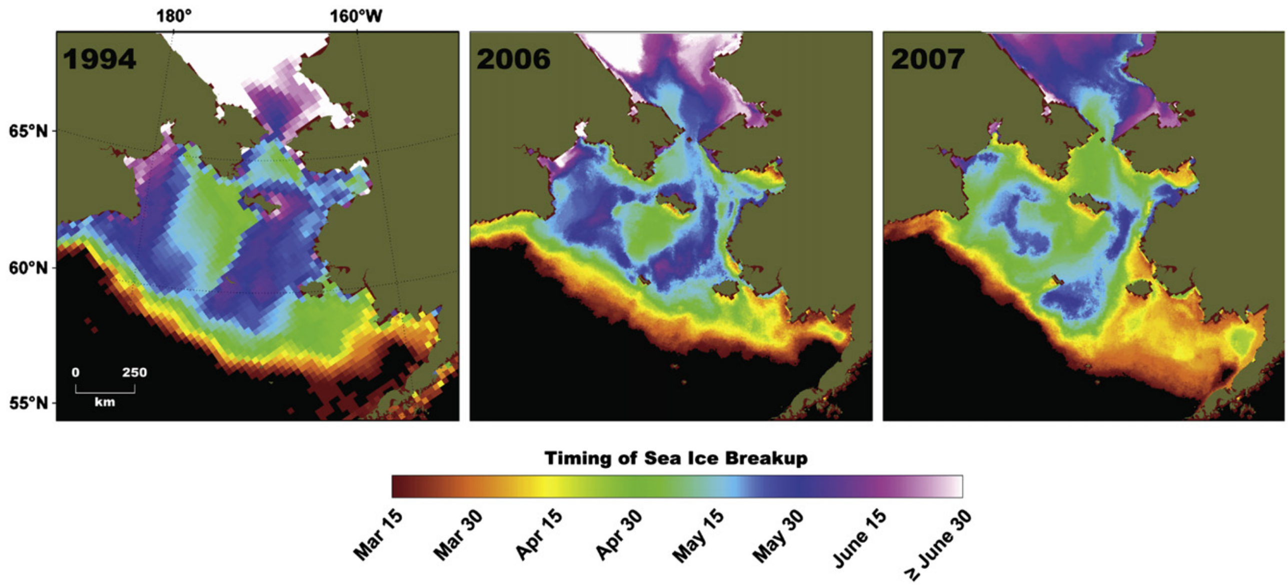

Fig. 14. Timing of sea ice retreat in 1994, 2006, and 2007, based on passive microwave satellite imagery, with the first day of sea ice concentrations below 15% considered the sea ice break-up date. Satellite data from 1994 are based on 25 km Special Sensor Microwave/Imager (SSM/I) sea ice concentrations available from the National Snow and Ice Data Center (www.nsidc.org). Satellite data from 2006 and 2007 are based on 6.25 km Advanced Microwave Scanning Radiometer for EOS (AMSR-E) sea ice concentrations available from the University of Hamburg (www.ifm.zmaw.de).

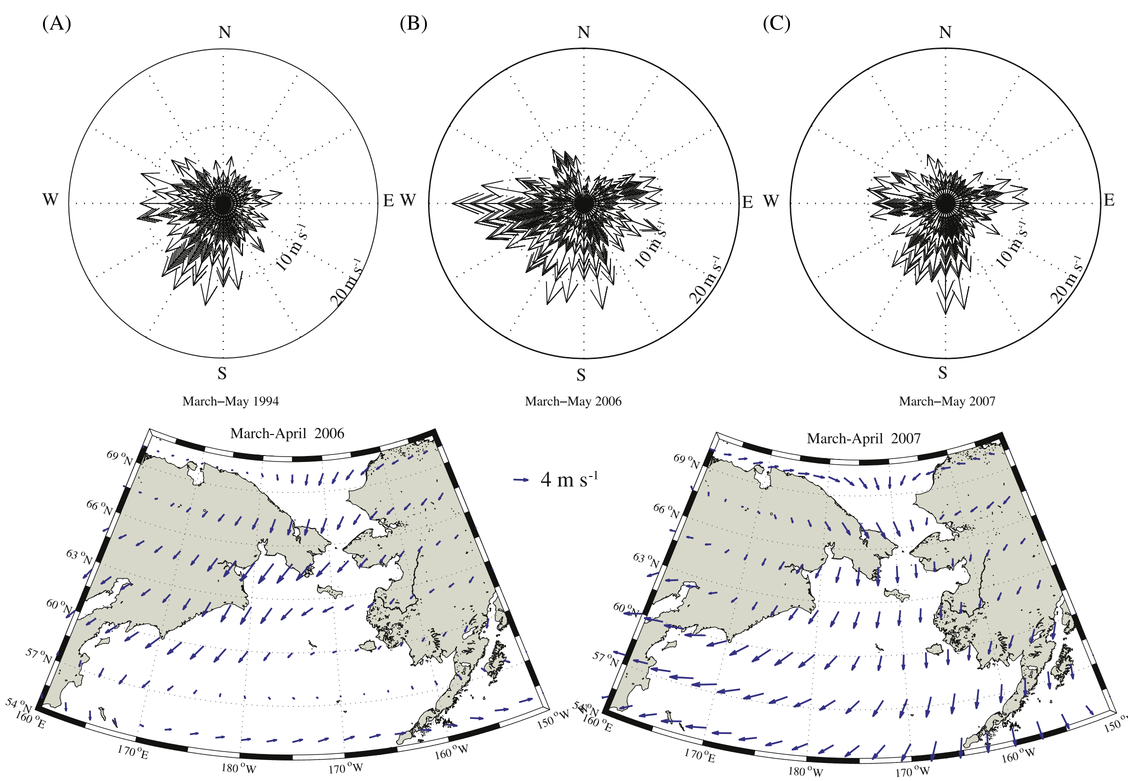

Fig. 15. Wind field intensity and vectors at the National Weather Service station at the Nome Airport from March through May, in 1994 (A), 2006 (B), and 2007 (C), based upon 3-h interval measurements (upper three panels). Arrows indicate the direction of surface winds relative to the four compass points, velocity is indicated by the length of the arrow. The highest winds during this period observed in 2006 were directed in a westerly direction (easterly origin), suggesting a linkage with the lower salinity, nutrients, and chlorophyll observed in May 2006. Mean March and April wind speed and direction from monthly mean NCEP winds over the Bering Sea in 2006 and 2007 (lower two map panels). The 2006 and 2007 wind comparison used the National Centers for Environmental Prediction (NCEP) reanalyzed estimates of zonal and meridional winds (http://www.esrl.noaa.gov/psd/data/reanalysis/reanalysis.shtml).

among the three years could be made are located primarily to the south and southwest of SLI. In all three years dissolution of sea ice occurred over roughly the same time period, from mid-April to mid-May, although ice retreat directly south of SLI clearly lagged into June during 1994. Given the prevailing northerly winds, open water to the south of SLI is commonly observed in the winter and

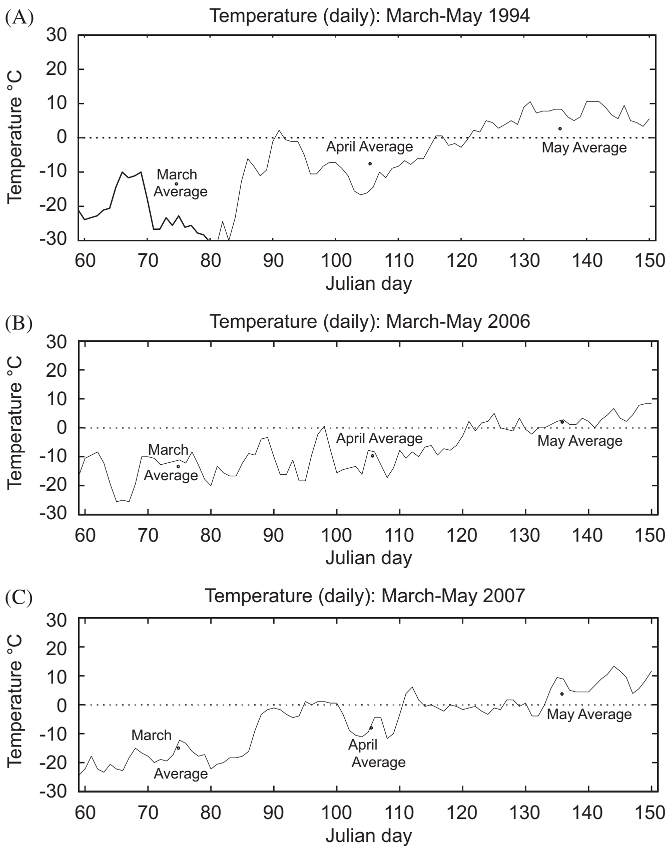

Fig. 16. Air temperatures observed at the Nome Airport, March–May 1994, 2006, and 2007. Sustained low air temperatures in March 2007 are hypothesized to be associated with high salinity water derived from brine injection that was observed in May 2007 on the eastern side of the Bering Sea (Fig. 5C and D), where typically low salinity Alaska Coastal Water predominates.

the transition to spring is often marked by the expansion of the wind-influenced winter polynya into a much larger spring open water feature with fringing, remnant ice to the south and east. One other significant difference among the three years was that in the most nutrient rich areas to the west of SLI and in the vicinity of Anadyr Strait, where both the highest nitrate and integrated chlorophyll was observed in 2007 (Figs. 4 and 7, respectively), sea ice breakup was up to several weeks earlier in 2007 and 1994 than it was in 2006. The direct linkage between the intense phytoplankton blooms immediately south of Bering Strait in both 2006 and 2007 and remnant sea ice drifting north also suggests that the timing of ice break-up does have influence on the timing of the spring bloom. However, other factors such as pre-formed nutrient content prior to significant biological production and related water mass boundaries as ice begins to break up have a strong influence on the bloom intensity.

3.6. *Atmospheric forcing*

While the predominant winds were northerly in 1994, 2006, and 2007 in the months leading up to sea ice break-up, more persistently northeasterly wind vectors were present in March–May 2006 (Fig. 15B) than were observed in either March-May 1994 (Fig. 15A) or March–May 2007 (Fig. 15C). Because the northern Bering Sea is largely confined by continental land masses, winds have a strong influence upon water mass boundaries (e.g. Cooper et al., 2006), and easterly and northeasterly wind vectors such as observed in 2006 might reasonably be expected to limit the eastward influence of high-nutrient AW. These winds, in turn, would have moved fresher and more nutrient-poor ACW across the shelf into the study region. The overall lower salinity and nutrient concentrations in spring 2006 are therefore consistent with prevailing winds having a significant influence on the less intensive bloom south of SLI that was observed in May 2006 relative to those in May 1994 or 2007.

Another factor that may have brought higher nutrient concentrations into the upper water column mixing was late winter brine formation that was clearly stronger in 2007 than in 2006. While direct measurements of nutrients are not available from the late winter months, brine injection with related vertical mixing would bring nutrients into surface waters from depth. The late winter months leading up to the 2007 bloom were characterized by sustained cold air temperatures that would have been conducive to sea-ice formation. For example, based upon US National Weather Service observations in Nome, Alaska (Fig. 16) air temperatures in March 2007 were much colder than average relative to March 2006. The impact of this cooling on northern Bering Sea waters would be to increase late winter sea ice formation, which has implications for bottom water formation and increased salinity through brine rejection, as observed in the bottom waters during May and June 2007. Furthermore, northerly winds in March 2007 (Fig. 15B) and anomalously cold conditions reduced coastal runoff and transport in the ACC, so that ACW remained confined on the eastern shelf. Hence, western Bering Sea water masses (i.e. AW) spread further east; the high nutrient content of these waters explains the higher salinity and nutrients than found in 2006.

4. Conclusions

In the northern Bering Sea, the proximity of land margins coupled with wind direction influences water mass boundaries between nutrient-rich AW and nutrient-poor ACW (Cooper et al., 2006). This can lead to different bloom intensities from conditions in the southern Bering Sea, where the timing of sea ice break-up is thought to have the strongest influence on the intensity of the bloom (e.g. Coyle et al., 2011; Hunt et al., 2002, 2011). The results of this study suggest that when the prevailing northerly winds have a significant easterly or northeasterly component in the weeks immediately prior to sea ice break-up such as in 2006 (Fig. 15B), more nutrient rich waters associated with the AW will be restricted towards the west and the overall intensity of the bloom in the northern Bering Sea will be lower (Fig. 4, Table 5). Several other factors may also influence the chlorophyll biomass in any particular year. We observed for example in 2006 that breakup of sea ice in the Anadyr Strait was several weeks later than in either 1994 or 2007 (Fig. 14), which were years when significantly higher chlorophyll biomass was observed. Given the link between sea ice breakup and the initiation of the annual ice edge bloom, it is possible that the lower chlorophyll biomass we observed in 2006 also resulted from late sea ice break-up in high nutrient waters near Anadyr Strait. We also observed evidence for greater brine injection prior to break-up in 2007 (Fig. 3), which could have provided for greater vertical mixing and potentially higher nutrient concentrations in surface waters.

Indicators of pelagic–benthic coupling such as the depth of the chlorophyll maximum, bottom water ammonium concentrations, sediment oxygen respiration rates, and surface sediment chlorophyll inventories show changes on this continental shelf on days-to-week timescales, as well as spatial complexity (Figs. 6, 9, 11, and 12). These dynamic changes over short-time periods indicate that caution is advised in sampling to adequately account for the processing of organic materials deposited to the benthos even within a single sea ice edge bloom. Other indicators that are not necessarily biologically based, such as the sedimentation of atmospherically-derived ^{7}Be, can show clear patterns of recent sedimentation in known areas of fine particle deposition on the sea floor on monthly or seasonal scales (Fig. 13). These areas of particle focusing are related to previously documented regions of high benthic biomass in finer, soft sediments (e.g. Grebmeier et al., 2006). This indicates that despite spatial and temporal variability in the sedimentation of labile materials to the benthos, physically-driven sedimentation and redistribution processes help to determine areas of high biomass and benthic productivity on the northern Bering Shelf.

Our observations suggest that conceptual models that link the timing of sea ice retreat to overall spring bloom production are likely to be insufficiently predictive in the northern Bering Sea. Interconnected complexities include increased seasonally open water in the Chirikov Basin over the past several decades, late winter brine injection, and wind forcing influences on west-to-east nutrient gradients. These factors represent some of the complexities preventing a straightforward interpretation of the influence of earlier ice retreat in the northern Bering Sea upon water column productivity and any resulting benthic ecosystem re-structuring in this subarctic-arctic boundary ecosystem.

Acknowledgments

The field sampling would not have been possible without strong support from the commanding officer, crew and officers of USCGC *Healy* on both the 2006 and 2007 cruises. Additional shipboard support was provided by Steve Roberts, Tom Bolmer, Susan Becker, and Scott Hiller. Similar thanks are extended to the commanding officer, crew and officers of the CCGS *Sir Wilfrid Laurier*. Also at sea, we thank Boris Sirenko, Adam Humphrey, Gay Sheffield, Marjorie Brooks, Mikhail Blikshteyn, Patricia Janes, Samantha Barlow, Kinuyo Kanamaru, Elizabeth Carvellas, Xuehua Cui, Beth Caissie, Kenna Wilkie, and Edward Davis for their help in collecting the data presented here. We also acknowledge the contributions of the late I.L. Larsen for his laboratory efforts that generated the ^{7}Be data. Alynne Bayard provided GIS expertise with drafting some of the figures. Financial support was primarily provided by the Office of Polar Programs of the National Science Foundation. We also acknowledge financial support by the North Pacific Research Board, and the Climate Observations Office of the National Oceanic and Atmospheric Administration. We thank two anonymous reviewers who provided constructive comments to improve an earlier version of the manuscript. BEST-BSIERP contribution 47. NPRB Publication 335.

References

Arrigo, K.R., van Dijken, G., Pabi, S., 2008. Impact of a shrinking Arctic ice cover on marine primary production. Geophys. Res. Lett. 35 (19), L19603. doi:10.1029/2008GL035028.

Brown, Z.W., van Dijken, G.L., Arrigo, K.R., 2011. A reassessment of primary production and environmental change in the Bering Sea. J. Geophys. Res. 116, C08014.

Clement, J.L., Cooper, L.W., Grebmeier, J.M., 2004. Late winter water column and sea ice conditions in the northern Bering Sea. J. Geophys. Res 109, C03022. doi:10.1029/2003JC002047. (C3).

Clement, J.L., Maslowski, W., Cooper, L.W., Grebmeier, J.M., Walczowski, W., 2005. Ocean circulation and exchanges through the northern Bering Sea—1979–2001 model results. Deep-Sea Res. II 52 (24–26), 3509–3540.

Cooper, L.W., Grebmeier, J.M., Larsen, I.L., Dolvin, S., Reed, A.J., 1998. Inventories and distribution of radiocessium in arctic marine sediments: influence of biological and physical processes. Chem. Ecol. 15, 27–46.

Cooper, L.W., Grebmeier, J.M., Larsen, I.L., Egorov, V.G., Theodorakis, C., Kelly, H.P., Lovvorn, J.R., 2002. Seasonal variation in sedimentation of organic materials in the St. Lawrence Island polynya region, Bering Sea. Mar. Ecol. Prog. Ser. 226, 13–26.

Cooper, L.W., Larsen, I.L., Grebmeier, J.M., Moran, S.B., 2005. Detection of rapid deposition of sea ice-rafted material to the Arctic Ocean benthos using the cosmogenic tracer ^{7}Be. Deep-Sea Res. II 52 (24–26), 3452–3461.

Cooper, L.W., Codispoti, L.A., Kelly, V., Sheffield, G., Grebmeier, J.M., 2006. The potential for using Little Diomede Island as a platform for observing environmental conditions in Bering Strait. Arctic 59 (2), 129–141.

Cooper, L.W., Lalande, C., C., Pirtle-Levy, R., Larsen, I.L., Grebmeier, J.M., 2009. Seasonal and decadal shifts in particulate organic matter processing and sedimentation in the Bering Strait Shelf Region. Deep-Sea Res. II 56, 1316–1325. doi:1310.1016/j.dsr1312.2008.1310.1025.

Cota, G.F., Smith, R.E.H., 1991. Ecology of bottom ice algae: II, dynamics, distributions and productivity. J. Mar. System 2, 279–295.

Coyle, K.O., Eisner, L.B., Mueter, F.J., Pinchuk, A.I., Janout, M.A., Cieciel, K.D., Farley, E.V., Andrews, A.G., 2011. Climate change in the southeastern Bering Sea: impacts on pollock stocks and implications for the oscillating control hypothesis. Fish. Oceanogr. 20 (2), 139–156.

Cui, X., Grebmeier, J.M., Cooper, L.W., Lovvorn, J.R., North, C.A., Seaver, W.L., Kolts, J.M., 2009. Spatial distributions of groundfish in the northern Bering Sea in relation to environmental variation. Mar. Ecol. Prog. Ser. 393, 147–160. doi:110.3354/meps08275.

Danielson, S., Aagaard, K., Weingartner, T., Martin, S., Winsor, P., Gawarkiewicz, G., Quadfasel, D., 2006. The St. Lawrence polynya and the Bering shelf circulation: new observations and a model comparison. J. Geophys. Res. 111 (C9), C09023.

Danielson, S., Eisner, L., Weingartner, T., Aagaard, K., 2011. Thermal and haline variability over the central Bering Sea shelf: seasonal and interannual perspectives. Cont. Shelf Res. doi:10.1016/j.csr.2010.12.010.

Grebmeier, J.M., Cooper, L.W., 1995. Influence of the St. Lawrence Island Polynya upon the Bering Sea Benthos. J. Geophys. Res. 100 (c3), 4439–4460.

Grebmeier, J.M., McRoy, C.P., 1989. Pelagic–benthic coupling on the shelf of the northern Bering and Chukchi Seas: III, benthic food supply and carbon cycling. Mar. Ecol. Prog. Ser. 53, 79–91.

Grebmeier, J.M., Feder, H.M., McRoy, C.P., 1989. Pelagic–benthic coupling on the Shelf of the Northern Bering and Chukchi Seas. II. Benthic community structure. Mar. Ecol. Prog. Ser. 51 (3), 253–268.

Grebmeier, J.M., Cooper, L.W., Feder, H.M., Sirenko, B.I., 2006. Ecosystem dynamics of the Pacific-influenced northern Bering, Chukchi, and East Siberian Seas. Prog. Oceanogr. 71, 331–361.

Grebmeier, J.M., Moore, S.E., Overland, J.E., Frey, K.E., Gradinger, R., R., 2010. Biological response to recent Pacific Arctic sea ice retreats. Eos Trans. AGU 91, 161–168. doi:10.1029/2010EO180001.

Hunt, G.L., Stabeno, P., Walters, G., Sinclair, E., Brodeur, R.D., Napp, J.M., Bond, N.A., 2002. Climate change and control of the southeastern Bering Sea pelagic ecosystem. Deep-Sea Res. II 49 (26), 5821–5853.

Hunt, G.L., Coyle, K.O., Eisner, L.B., Farley, E.V., Heintz, R.A., Mueter, F., Napp, J.M., Overland, J.E., Ressler, P.H., Salo, S., Stabeno, P., 2011. Climate impacts on eastern Bering Sea foodwebs: a synthesis of new data and an assessment of the Oscillating Control Hypothesis. ICES J. Mar. Sci., doi:10.1093/icesjms/fsr036.

Kanneworff, E., Nicolaisen, W., 1973. The "HAPS:" A frame supported bottom corer. Ophelia Suppl. 10, 119–129.

Kinder, T.H., Coachman, L.K., Galt, J.A., 1975. The Bering slope current system. J. Phys. Oceanogr. 5 (4), 231–244.

Lomas, M.W., Moran, S.B., Casey, J.R., Bell, D.W., Tiahlo, M., Whitefield, J., Kelly, R.P., Mathis, J.T., Cokelet, E.D., 2012. Spatial and seasonal variability of primary production on the Eastern Bering Sea shelf. Deep-Sea Res. II 65–70, 126–140.

Lovvorn, J.R., Cooper, L.W., Brooks, M.L., De Ruyck, C.C., Bump, J.K., Grebmeier, J.M., 2005. Organic matter pathways to zooplankton and benthos under pack ice in late winter and open water in late summer in the north-central Bering Sea. Mar. Ecol. Prog. Ser. 291, 135–150.

McRoy, C.P., 1993. ISHTAR, the project: an overview of Inner Shelf Transfer and Recycling in the Bering and Chukchi seas. Cont. Shelf Res. 13, 473–479.

McRoy, C.P., Hood, D.W., Coachman, L.K., Walsh, J.J., Goering, J.J., 1986. Processes and resources of the Bering Sea Shelf (PROBES): the development and accomplishments of the project. Cont. Shelf Res. 5 (1/2), 5–21.

Mordy, C.W., Stabeno, P.J., Ladd, P.J., Zeeman, C., Wisegarver, S., Salo, D.P., Hunt, S., G.L., 2005. Nutrients and primary production along the eastern Aleutian Island Archipelago. Fish. Oceanogr. 14, 55–76.

Niebauer, H.J., 1991. Bio-physical oceanographic interactions at the edge of the Arctic ice pack. J. Mar. System 2, 209–232.

Niebauer, H.J., Alexander, V., Heinrichs, S.M., 1995. A time series study of the spring bloom at the Bering Sea ice edge, I: physical processes, chlorophyll and nutrient chemistry. Cont. Shelf Res. 15, 1859–1877.

Pirtle-Levy, R., Grebmeier, J.M., Cooper, L.W., Larsen, I.L., 2009. Seasonal variation of chlorophyll *a* in Arctic sediments implies long persistence of plant pigments. Deep-Sea Res. 56 (2009), 1326–1338.

Pyenson, N.D., Lindberg, D.R., 2011. What happened to gray whales during the Pleistocene? The ecological impact of sea-level change on benthic feeding areas in the North Pacific Ocean. PLoS One 6 (7), e21295. doi:10.1371/journal.pone.0021295.

Springer, A.M., McRoy, C.P., Flint, M.V., 1996. The Bering Sea Green Belt: shelf-edge processes and ecosystem production. Fish. Oceanogr. 5 (3–4), 205–223.

Stabeno, P.J., Farley, E., Kachel, N., Moore, S., Mordy, C., Napp, J.M., Overland, J.E., Pinchuk, A.I., Sigler, M.F., 2012. A comparison of the physics of the northern and southern shelves of the eastern Bering Sea and some implications for the ecosystem. Deep-Sea Res. II 65–70, 14–30.

Stringer, W.J., Groves, J.E., 1991. Location and areal extent of polynyas in the Bering and Chukchi Seas. Arctic 44, 164–171.

Walsh, J.J., McRoy, C.P., Coachman, L.K., Goering, J.J., Nihoul, J.J., Whitledge, T.E., Blackburn, T.H., Parker, P.L., Wirick, C.D., Shuert, P.G., Grebmeier, J.M., Springer, A.M., Tripp, R.D., Hansell, D.A., Djenidi, S., Deleersnijder, E., Henricksen, K., Lund, B.A., Andersen, P., Müller-Karger, F.E., Dean, K., 1989. Carbon and nitrogen cycling within the Bering/Chukchi Seas: source regions for organic matter effecting AOU demands of the Arctic Ocean. Prog. Oceanogr. 22, 277–359.

Wang, J., Hu, H., Mizobata, K., Saitoh, S., 2009. Seasonal variations of sea ice and ocean circulation in the Bering Sea: a model-data fusion study. J. Geophys. Res. 14, C02011.

Welschmeyer, N.A., 1994. Fluorometric analysis of chlorophyll a in the presence of chlorophyll *b* and pheopigments. Limnol. Oceanogr 39, 1985–1992.